

Identification and control of systems with hysteresis: concepts and tools

Petrus Emmanuel Oliveira Gomes Brant Abreu*

Programa de Pós-Graduação em Engenharia Elétrica,
Universidade Federal de Minas Gerais,
Av. Antônio Carlos 6627, 31270-901,
Belo Horizonte, MG, Brazil
Email: petrusabreu@ufmg.br

*Corresponding author

Henrique Carvalho de Castro

Programa de Pós-Graduação em Engenharia de Sistemas e Automação,
Universidade Federal de Lavras,
Campus Universitário, P.O. 3037, 37200-000,
Lavras, MG, Brazil
Email: henriquec.castro@outlook.com

Bruno Henrique Groenner Barbosa

Departamento de Automática,
Universidade Federal de Lavras,
Campus Universitário, P.O. 3037, 37200-000,
Lavras, MG, Brazil
Email: brunohb@ufla.br

Luis Antonio Aguirre

Departamento de Engenharia Eletrônica,
Universidade Federal de Minas Gerais,
Av. Antônio Carlos 6627, 31270-901,
Belo Horizonte, MG, Brazil
Email: aguirre@ufmg.br

Abstract: Nonlinear system identification and control is a very vast field. In order to make a brief review manageable the topic has been constrained to focus on systems with hysteresis. The model class that received most attention was that of nonlinear autoregressive with exogenous (NARX) inputs polynomial models. However, most of the problems mentioned and tools presented are applicable to a much wider class of nonlinear systems. A framework for nonlinear system identification based on evolutionary algorithms is described. Identification and control of systems with hysteresis are illustrated with examples that include simulated and experimental data. Some open problems in the field are mentioned and it is hoped that this work will not only serve as a starting point for the newcomer but also motivate researchers to face open challenges.

Keywords: grey-box identification; compensation of nonlinearities; NARX polynomial models; hysteresis; evolutionary algorithms; multi-gene genetic programming; MGGP.

Reference to this paper should be made as follows: Abreu, P.E.O.G.B., de Castro, H.C., Barbosa, B.H.G. and Aguirre, L.A. (2024) 'Identification and control of systems with hysteresis: concepts and tools', *Int. J. Modelling, Identification and Control*, Vol. 44, No. 3, pp.189–217.

Biographical notes: Petrus Emmanuel Oliveira Gomes Brant Abreu received a BSc in Control and Automation Engineering in 2012 from the Faculdade de Ciências e Tecnologia de Montes Claros, Brazil, a specialisation in Systems Engineering in 2015 from the Universidade Estadual de Montes Claros, Brazil, MSc and DSc in Electrical Engineering from the Universidade Federal de Minas Gerais, Brazil, respectively in 2016 and 2021. He is currently a Temporary Professor at the Department of Control, Automation and Computing Engineering at the Universidade Federal de Santa Catarina. His research includes the identification of nonlinear systems, nonlinear dynamics, control systems, and time-varying dynamic systems.

Henrique Carvalho de Castro received his BSc in Control and Automation Engineering in 2017 from the Universidade Federal de Lavras (UFLA), Brazil, a MSc in Systems and Automation Engineering in 2021 from the UFLA. He is currently pursuing a DSc in Electrical Engineering from the Universidade Federal de Minas Gerais. His research includes the evolutionary computing, identification of nonlinear systems, and nonlinear dynamics.

Bruno Henrique Groenner Barbosa received his BSc in Control and Automation Engineering, and MSc and DSc in Electrical Engineering from the Federal University of Minas Gerais, Brazil, in 2003, 2006, and 2009, respectively. In 2008, he was a visiting researcher with the University of New South Wales, Australia. In 2020, he was a Visiting Professor with the Department of Mechanical and Mechatronics Engineering, University of Waterloo, Canada. He is an Associate Professor with the Department of Automatics, Federal University of Lavras, Brazil, where he heads the Artificial Intelligence and Automation Research Group. His research interests include artificial intelligence techniques, such as neural networks and evolutionary algorithms, for solving real-world engineering problems. These have included identification of nonlinear dynamical systems, development of soft sensors, pattern recognition, systems optimisation, and control.

Luis Antonio Aguirre received his PhD in 1994 from the University of Sheffield, England. He joined the Department of Electronics Engineering at UFMG in 1995 where he currently serves as a Full Professor. He is an author of five books and was the Editor-in-Chief of *Encyclopédia de Automática* (three volume set), sponsored by the Brazilian Society of Automation (SBA) and published by Editora Blücher. From 2009 to 2012 he served as the Editor-in-Chief of *Controle & Automação: Revista da Sociedade Brasileira de Automática*, currently published by Springer Verlag under the name *Journal of Control, Automation and Electrical Systems*. His research includes the identification of nonlinear system, grey-box identification, nonlinear dynamics, and analysis of dynamical networks.

1 Introduction

Mathematical modelling of dynamical systems concerns the area of knowledge that deals with techniques developed to describe the behaviour of real systems using models. In general, the related techniques can be grouped into two frameworks, one based on *first principles* and the other based on *empirical data*. The former leads to models where the parameters typically have physical meaning. Unfortunately, the development of such models, whenever viable, is time consuming and their use in model-based control or compensation design is rather hard due to their structural complexity (Peng and Chen, 2013; Hassani et al., 2014). On the other hand, when models are built directly from data, it is often possible to choose a model structure that is more suitable for control or compensation purposes. Such techniques are part of a mature field known as *system identification* (Ljung, 1999; Isermann and Münchhof, 2011; Billings, 2013).

Most experimental systems have some level of nonlinear and time-varying behaviour (Bequette, 1991; Gebraad et al., 2013; Choudhury et al., 2008; Koo, 1995; Stebel and Czeczot, 2009). Nonlinear systems are often classified as systems with *hard* or *severe nonlinearities* such as friction (Romano and Garcia, 2011; Baeza and Garcia, 2018; Nnaji et al., 2021), dead-zone (Aguirre, 2014), dead-band (Choudhury et al., 2008), hysteresis (Morris, 2011) and those related to pH neutralisation (Bhadra et al., 2019b; Abreu et al., 2021; Wei et al., 2021), which tend to present considerable challenges for identification and control purposes (Tao and Kokotovic, 1995; Choudhury

et al., 2008; Visone, 2008; Billings, 2013; Biagiola et al., 2016; Pop et al., 2018). Some examples include mechanical, electronic, biomedical and pH neutralisation processes, as well as sensors and actuators such as pneumatic control valves and piezoelectric actuators (PEAs) (Choudhury et al., 2008; Stebel and Czeczot, 2009; Peng and Chen, 2013; Rakotondrabe, 2013). One of the aims of this paper is to briefly mention the identification of such systems, with special emphasis on systems with hysteresis.

The field of nonlinear system identification has developed two classes of techniques called *black-box* and *grey-box*. These terms should refer to the techniques rather than to model representations. That is, the same model class can be developed using black-box or grey-box methods. In black-box modelling, it is assumed that the only available source of information about the system is the input and output data. While in the realm of grey-box techniques *auxiliary information* about the system is available and used in addition to the dynamical data (Aguirre, 2019). A pioneering publication on the use of auxiliary information in system identification is (Eskinat et al., 1993). The inclusion of such information often improves performance by enabling the model to have features that are not ensured by black-box techniques (Sjöberg et al., 1995). Some ways to achieve this for hysteretic systems will be discussed in the present paper.

The identification of nonlinear dynamical models is a challenging problem that can be decomposed into two subtasks: model structure selection and parameter estimation. In this context, a convenient model representation is the nonlinear autoregressive

with exogenous (NARX) inputs polynomial model (Leontaritis and Billings, 1985a, 1985b), which consists of a recursive input-output expression composed of a nonlinear polynomial function of lagged inputs and outputs. However, identifying the correct structure for such a representation, which can be seen as a combinatorial optimisation problem, is not a simple task.

Most identification methods in the literature concerning NARX models suffer from the dimensionality problem with the increment of nonlinearity degree and long-term dependencies. Thus, we present in this work a metaheuristic tool called *multi-gene genetic programming* (MGGP) (Hinchliffe and Willis, 2003; Castro and Barbosa, 2022) capable of concomitantly create and select the model regressors. A case study is presented where the implemented MGGP is used to identify a PEA (Rakotondrabe, 2011) using auxiliary information about the hysteretic nonlinearity inherent to such actuators, hence constituting a grey-box technique. It is also shown that the way the model is simulated during the structure selection task is critical in finding models that correctly represent the system hysteresis.

A related topic of interest is model-based control (Hong et al., 1996; Ikhouane and Rodellar, 2007; Abdullah et al., 2012; Esbrook et al., 2013; Chaoui and Gualous, 2016; Bhadra et al., 2019a; Larico and Garcia, 2019; Lacerda Júnior et al., 2019; Ji et al., 2021) and compensation (Visone, 2008; Al Janaideh et al., 2011; Qin et al., 2013; Chaoui and Gualous, 2016; Yi et al., 2019; Abreu et al., 2020; Abreu, 2021; Tavares et al., 2022) that tend to cancel or compensate for the system nonlinearity. In this context, the use of NARX polynomial models presents some advantages due to their ability to represent a wide class of nonlinear behaviours (Leontaritis and Billings, 1985a, 1985b) and their structural flexibility which, when combined with grey-box identification techniques (Aguirre, 2019), are promising for their use in control or compensation (Pearson, 1999).

The paper is organised as follows. Approaches to modelling systems with hysteresis are addressed in Section 2. A set of general tools for nonlinear system identification is briefly presented in Section 3. Section 4 discusses control and compensation schemes with special emphasis on hysteretic systems. The paper ends with conclusions in Section 5.

2 Modelling of hysteretic systems

Hysteresis is commonly related to phenomena such as ferromagnetism, plasticity, and friction, among others (Visintin, 1994). Some examples include mechanical, electronic and biomedical systems, as well as sensors and actuators such as magneto-rheological dampers, PEAs and pneumatic control valves (Choudhury et al., 2008; Rakotondrabe, 2013; Peng and Chen, 2013). An intrinsic feature of such systems is the memory effect, meaning that the output depends on the history of the corresponding input.

Hysteresis has been associated with the existence of several fixed points whenever these systems are subject to constant (Morris, 2011) or time-varying (Martins and Aguirre, 2016) input signals. The representation of such phenomenon has been addressed using phenomenological models and by means of models built from data, as briefly surveyed in what follows.

2.1 Phenomenological models

In the realm of *models based on first principles*, contributions include differential equations and operators (Hassani et al., 2014), such as the Bouc-Wen model (Wen, 1976), the Duhem model (Oh and Bernstein, 2005), the Preisach model (Ge and Jouaneh, 1996) and the Prandtl-Ishlinskii operator (Brokate and Sprekels, 1996). These models, that are known to be challenging for system identification techniques (Quaranta et al., 2020), have been widely used to represent a variety of hysteresis loops that resemble real nonlinear hysteretic systems (Smyth et al., 2002). In some cases, as for the Bouc-Wen model that has a well known structure, the challenge stems from the problem of estimating its parameters, which appear nonlinearly in the equation. This has led many works in the literature to focus on how to estimate the parameters of such a model, which often requires sophisticated optimisation algorithms (Kyriianou et al., 2001; Worden and Hensman, 2012; Carboni et al., 2018). Apart from the computational effort required in the identification of phenomenological models, their application in the design of compensators is somewhat limited due to their structural complexity (Peng and Chen, 2013; Hassani et al., 2014).

Pioneering works that addressed the hysteresis phenomenon, through a functional, were developed by Robert Bouc who proposed to describe hysteresis with (Bouc, 1971):

$$\dot{\mathcal{F}}(t) = g(x(t), \mathcal{F}(t), \text{sign}(\dot{x}(t)))\dot{x}(t), \quad (1)$$

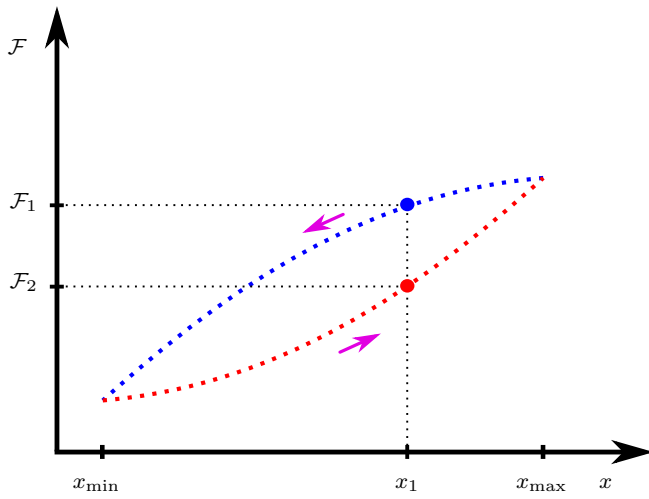
where $g(\cdot)$ is a nonlinear mapping, $x(t)$ is a displacement, $\mathcal{F}(t)$ represents a resultant force, and the $\text{sign}(\cdot) : \mathbb{R} \rightarrow \mathbb{R}$ function defined as (Popiolek, 1990):

$$\text{sign}(x) = \begin{cases} 1, & \text{if } x > 0; \\ -1, & \text{if } x < 0; \\ 0, & \text{if } x = 0. \end{cases} \quad (2)$$

Functional (1) describes the relationship between the forced vibrations of a hysteretic system under periodic excitation (Sain et al., 1998), as illustrated in Figure 1.

Bouc (1971) assumed that the shape of the hysteresis loop, in Figure 1, remains the same for any input frequency, which refers to the *rate-independent property*. Rate-independent hysteresis is a dominant feature under low-frequency excitation (Visintin, 1994; Mayergoz, 2003; Ikhouane and Rodellar, 2007; Morris, 2011; Cao et al., 2013) and the hysteresis loop does not vanish when the input frequency approaches zero (Bernstein, 2007).

Figure 1 Schematic representation of the input-output relationship in a hysteresis loop indicated with (.....) (see online version for colours)



Notes: For an input value x_1 , there are two output values \mathcal{F}_1 (●) and \mathcal{F}_2 (●), which depend on the input change indicated with (→).

The class of dynamical systems studied by Bouc (1971) can be represented as:

$$\ddot{x}(t) + \mathcal{F}(t) = p(t), \quad (3)$$

where $p(t)$ refers to system input. Bouc (1971) also proposed a variant of the Stieltjes integral for the output \mathcal{F} , such that equations (1) and (3) could be rewritten as:

$$\ddot{x}(t) + \mu^2 x(t) + \sum_{i_h=1}^{N_{i_h}} h_{i_h}(t) = p(t), \quad (4)$$

$$\dot{h}_{i_h}(t) + \beta_{i_h} |\dot{x}(t)| h_{i_h}(t) - A_{i_h} \dot{x}(t) = 0, \quad i_h = 1, \dots, N_{i_h}, \quad (5)$$

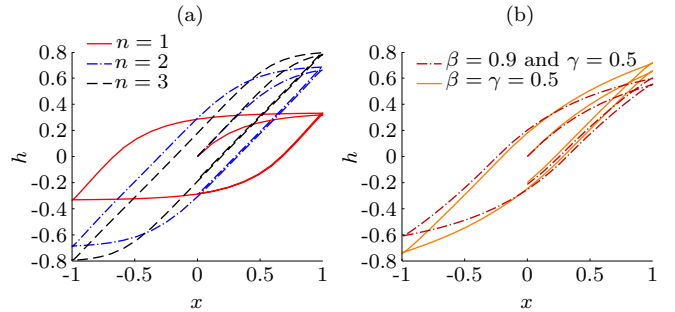
for which h_{i_h} corresponds to the hysteretic behaviour of the N_{i_h} restoring forces acting on the system, whose constant coefficients μ , β_{i_h} and A_{i_h} must be estimated. Models (4) and (5) are known as the Bouc model. Wen (1976) extended model (5) giving rise to the so-called Bouc-Wen model expressed as:

$$\dot{h}(t) = A \dot{x}(t) - \beta |\dot{x}(t)| |h(t)|^{n-1} h(t) - \gamma \dot{x}(t) |h(t)|^n, \quad (6)$$

such that $h(t)$ determines the hysteresis output, $x(t)$ is the model input. The scale and general shape of the hysteresis loop are determined by A , β and γ , while its smoothness is adjusted by n (Ikhouane and Rodellar, 2007; Wang and Zhu, 2011); see Figure 2. An in-depth analysis of this model, which is widely used in the literature (Domínguez-González et al., 2014; Ahmad, 2018), can be found in Ismail et al. (2009) and Charalampakis (2010).

Parameter estimation applied to the Bouc-Wen model has been discussed in Ha et al. (2005), Hassani et al. (2014) and Wei et al. (2014) and issues related to the modelling and control of dynamical systems that include this type of hysteresis is presented in Ikhouane and Rodellar (2007) and Ismail et al. (2009).

Figure 2 Illustration of different hysteresis loops of the Bouc-Wen model (6), (a) the effect of n on hysteresis loop for $A = 1$, $\beta = 1$, $\gamma = 2$ and $n = \{1, 2, 3\}$, while in (b) the hysteresis loops for $n = 1$ and $A = 1$ with $\beta = \gamma = 0.5$ and $\beta = 0.9$ and $\gamma = 0.5$ (see online version for colours)



Notes: The input signal is $x(t) = \sin(2\pi ft)$ with $f = 1$ Hz.

Another way of modelling hysteresis is by means of operators (Zakerzadeh et al., 2011) as proposed in the early 1970's by Mark Alexandrovich Krasnosel'skii and co-workers (Visintin, 1994). One of the most popular operator-based models used to characterise hysteresis behaviour is the Preisach model (Hu and Ben Mrad, 2003). From this model, two operator-based models can be derived, the Krasnosel'skii-Pokrovskii (KP) and the Prandtl-Ishlinskii models (Banks et al., 1997; Hassani et al., 2014; Gu et al., 2012).

The Prandtl-Ishlinskii model is defined as the sum of several weighted elementary operators, also called *play operators* (Kuhnen, 2003). Each of these operators is parameterised by a radius r_{aj} . The j^{th} play operator $P_{r_{aj}}$ for input $u(t)$ is (see Figure 3) defined as:

$$\nu_{r_{aj}}(t) = \max(\min(u(t) + r_{aj}, \nu_{r_{aj}}(t^-)), u(t) - r_{aj}), \\ \triangleq P_{r_{aj}}(u(t); \nu_{r_{aj}}(t^-)), \quad (7)$$

for which $\nu_{r_{aj}}(t)$ and $\nu_{r_{aj}}(t^-)$ are, respectively, the current and previous state of the play operator.

For each play operator, there are two possible modes in which its state can be found at time t , one corresponds to the linear region, such that $\nu_{r_{aj}}(t) = u(t) \pm r_{aj}$, illustrated by blue continuous lines in Figure 3. The other mode is called the play region, where the state is constant, given by $\nu_{r_{aj}}(t) = \nu_{r_{aj}}(t^-)$ and indicated by dashed lines in Figure 3 (Esbrook et al., 2014).

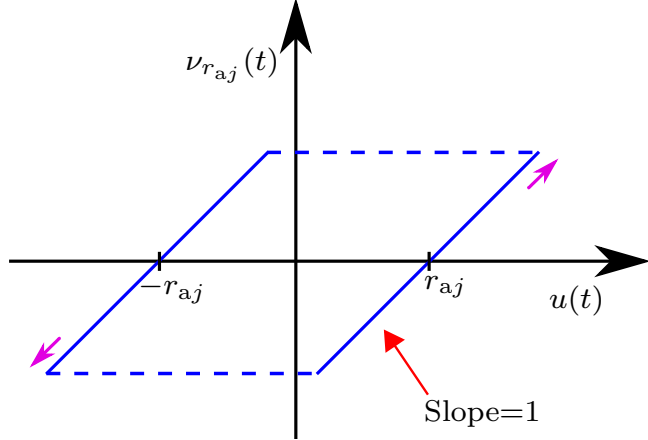
For the case of n_r play operators $P_{r_{aj}}$ (7), a Prandtl-Ishlinskii operator output $H(\cdot)$ is given by:

$$\nu(t) = H(u(t); \nu_{r_a}(t^-)) \\ = \sum_{j=1}^{n_r} \theta_j P_{r_{aj}}(u(t); \nu_{r_{aj}}(t^-)), \quad (8)$$

where $\nu_{r_a}(t) \triangleq [\nu_{r_{a1}}(t) \nu_{r_{a2}}(t) \dots \nu_{r_{an_r}}(t)]^T$ is the vector composed of the state variables $\nu_{r_{aj}}(t)$, of the n_r play operators, at the current time t , and $\nu_{r_a}(t^-) \triangleq [\nu_{r_{a1}}(t^-) \nu_{r_{a2}}(t^-) \dots \nu_{r_{an_r}}(t^-)]^T$ is the vector of state

variables at the instant immediately preceding the current time. Each weight θ_j is assumed to be bounded, non-negative and greater than zero, while the radii r_{aj} satisfy the following condition: $0 = r_{a1} < r_{a2} < \dots < r_{an_r} < \infty$ (Esbrook et al., 2014).

Figure 3 Play operator (see online version for colours)



Notes: $u(t)$ is the input signal, and $\nu_{r_{aj}}(t)$ represents the state values of the j^{th} operator.

In order to rewrite (8) in a compact form, one can define $\mathcal{P} \triangleq [P_{r_{a1}} P_{r_{a2}} \dots P_{r_{an_r}}]^T$, which represents the temporal evolution of states $\boldsymbol{\nu}_{r_a}(t)$ of (8) with respect to input $u(t)$, such that:

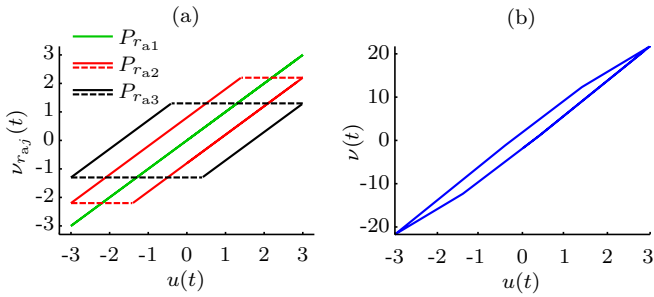
$$\boldsymbol{\nu}_{r_a}(t) = \mathcal{P}(u(t); \boldsymbol{\nu}_{r_a}(t^-)). \quad (9)$$

Furthermore, $\boldsymbol{\theta} \triangleq [\theta_1 \theta_2 \dots \theta_{n_r}]^T$ and $\mathbf{r}_a \triangleq [r_{a1} r_{a2} \dots r_{an_r}]^T$. Thus, one can represent the output of the Prandtl-Ishlinskii operator (8) as (see Figure 4):

$$\nu(t) = H(u(t); \boldsymbol{\nu}_{r_a}(t^-)) = \boldsymbol{\theta}^T \boldsymbol{\nu}_{r_a}(t). \quad (10)$$

More details on Prandtl-Ishlinskii models can be found in Visintin (1994) and Brokate and Sprekels (1996).

Figure 4 Illustration of an operator (10) with $n_r = 3$, with radii given by $\mathbf{r}_a = [0 \ 0.8 \ 1.7]^T$ and weighted by $\boldsymbol{\theta} = [5.88 \ 1.58 \ 0.47]^T$, (a) output of the operators $P_{r_{a1}}$, $P_{r_{a2}}$ and $P_{r_{a3}}$ (b) the hysteresis loop for $u(t) = 3 \sin(2\pi ft)$ with $f = 1$ Hz (see online version for colours)



2.2 NARX models

The NARX inputs representation is considered a convenient choice due to its ability to predict a wide class of nonlinear behaviours, which is given by (Leontaritis and Billings, 1985a, 1985b; Billings, 2013):

$$y_k = F(y_{k-1}, \dots, y_{k-n_y}, u_{k-\tau_d}, \dots, u_{k-n_u}), \quad (11)$$

where $y_k \in \mathbb{R}$ is the output at instant $k \in \mathbb{N}$, and $u_k \in \mathbb{R}$ is the input signal, which are obtained by measuring the continuous data $y(t)$ and $u(t)$ at sampling intervals T_s , respectively, and $\tau_d \in \mathbb{N}^+$ is the pure time delay. Moreover, n_y and n_u are the maximum lags for the output and input, respectively, and $F(\cdot)$ is a nonlinear function of the lagged outputs and inputs.

The NARX philosophy concerns not only obtaining models that closely fit the behaviour of the investigated systems, but that can also be used to help understand the dynamical properties (Aguirre and Billings, 1995; Aguirre and Mendes, 1996; Pearson, 1999). This identification framework was developed in a black-box setting (Sjöberg et al., 1995; Chan et al., 2015; Ayala et al., 2015; Fu et al., 2016; Trivedi and Rawat, 2022) but is well suited to grey-box approaches as presented in Aguirre (2019) and references therein.

In the context of hysteretic systems, the use of NARX models that are especially dedicated to the description of such systems and/or that can be effectively used to design compensators that mitigate their hysteresis nonlinearity is an open and recent branch of research, whose results are still scarce in the literature (Deng and Tan, 2009; Dong and Tan, 2014; Martins and Aguirre, 2016; Lacerda Júnior et al., 2019; Abreu, 2021). Some of the qualitative behaviours that NARX models, especially in polynomial form, may exhibit are: input amplitude-dependent stability, super and subharmonic generation, asymmetric responses to symmetric input changes, and output multiplicity (Pearson, 1999; Deng and Tan, 2009; Martins and Aguirre, 2016; Fujii et al., 2018).

In terms of data fitting, NARX neural networks are an excellent choice due to their property of universal approximators, which leads to models with good performance for predicting nonlinear systems (Barbosa et al., 2011; Chan et al., 2015; Fu et al., 2016). On the other hand, the use of NARX polynomial models has been argued to be an appealing way, since it may be possible to achieve good performance with far less parameters (Aguirre et al., 2002; Martins and Aguirre, 2016; Lacerda Júnior et al., 2019; Abreu, 2021). From now on, NARX polynomial models will be considered as the model class (Chen and Billings, 1989).

It will be useful for our purposes to rewrite a NARX model as (Abreu et al., 2020; Abreu, 2021):

$$y_k = F^\ell(y_{k-1}, \dots, y_{k-n_y}, u_{k-\tau_d}, \dots, u_{k-n_u}, \phi_{i,k-1}, \dots, \phi_{i,k-n_{\phi_i}}), \quad (12)$$

where n_{ϕ_i} is the maximum lag considered for the i^{th} specific function that can optionally be included as a

candidate regressor in the model, represented by $\phi_{i,k}$, $F^\ell(\cdot)$ is a polynomial function of the regressor variables up to degree $\ell \in \mathbb{N}^+$, and the other variables are the same as defined in equation (11). The additional term $\phi_{i,k}$ is commonly defined as a function of lagged values of y_k and u_k , e.g., $\phi_{1,k} = u_k - u_{k-1}$, (Billings and Chen, 1989a; Leva and Piroddi, 2002; Khalid et al., 2014; Martins and Aguirre, 2016). The goal is to choose functions $\phi_{i,k}$ that allow the models to predict systems whose nonlinearities cannot be well approximated using only regressors based on monomials of lagged input and output values. Thus, a relevant question arises: *how to determine, or which are, such functions?*

As an example, consider the absolute value $|\cdot|$ of a real number x that can be expressed as the product of this real number and its sign function (Popiołek, 1990), such that: $|x| = x \cdot \text{sign}(x)$. Hence, a discrete counterpart of the Bouc-Wen model (6), using y_k and u_k to refer to the output and input of the model, can be rewritten as:

$$\begin{aligned} y_k = & y_{k-1} + A \underbrace{[u_k - u_{k-1}]}_{\phi_{1,k}} \\ & - \beta [u_k - u_{k-1}] \underbrace{\text{sign}(u_k - u_{k-1}) y_{k-1}}_{\phi_{2,k}} \\ & - \gamma [u_k - u_{k-1}] \underbrace{\text{sign}(y_{k-1}) y_{k-1}}_{\phi_{3,k}}, \end{aligned} \quad (13)$$

where it is shown how some $\phi_{i,k}$ naturally appear and could be used in determining the structure of a hysteretic model. Another example has been provided in Abreu et al. (2021), in modelling a pH neutralisation process from experimental data, where:

$$\dot{y}(t) \approx \frac{y_{kT_s} - y_{[k-1]T_s}}{T_s} = \phi_{1,k}, \quad (14)$$

was proposed to improve the ability of the identified NARX models to describe varying behaviour.

The main steps in a typical system identification problem are:

- 1 *Dynamic testing*, where special attention should be paid to the use of *persistently exciting input signals* (Schoukens and Ljung, 2019; Tavares et al., 2021; Abreu, 2021) and a proper choice of the sampling time (Billings and Aguirre, 1995; Lacerda Júnior et al., 2017).
- 2 *Choice of model class*, here we focus on NARX polynomials (Billings, 2013).
- 3 *Structure selection*, where the regressor variables in equation (12) should be carefully chosen (Billings et al., 1989; Aguirre and Billings, 1995; Piroddi and Spinelli, 2003; Hong et al., 2008; Piroddi, 2008; Wei and Billings, 2008; Baldacchino et al., 2013; Shi and Wu, 2013; Falsone et al., 2015; Bianchi et al., 2016; Retes and Aguirre, 2019; Bianchi et al., 2021; Fagundes et al., 2022).

4 *Parameter estimation*, that can be achieved in batch (Ljung, 1999; Nelles, 2001; Isermann and Münchhof, 2011) or recursively (Paleologu et al., 2008; Keesman, 2011; Beza and Bongiorno, 2014).

5 *Model validation*, where a number of procedures are available (Haynes and Billings, 1992; Aguirre and Billings, 1994; Billings and Zheng, 1999; Letellier et al., 2002; Billings, 2013).

2.2.1 Black-box approaches

Few works consider NARX models, especially in polynomial form, in the representation of hysteresis, and in most cases the approach is black-box and structure selection is mostly *ad hoc*. For instance, in Parlitz et al. (2004) a model with 32 terms was estimated, in Worden et al. (2007) a model with 84 terms was estimated and in Karami et al. (2021) the model had 196 terms. Zhang et al. (2017a), in turn, proposed a new truncation condition to be assumed during the structure selection step, whose models were estimated with about 11 terms.

Related work was performed by Masri and co-workers using continuous-time polynomials in a black-box fashion (Masri et al., 2004). As with the previous papers, the authors set off with a large model either 22 or 42 terms and prune it at a latter stage. The need for a more careful structure selection procedure was acknowledged by the authors. The authors in Brewick et al. (2016) use Chebyshev polynomials and point out that very compact models were possible to be obtained at the cost of some performance. When models are built to closely fit the collected dataset (Chan et al., 2015; Ayala et al., 2015; Fu et al., 2016) certain features of hysteretic system cannot be guaranteed. Results in the field of neural networks can be found in Zhang et al. (2010), Wang and Song (2014) and Wang et al. (2020).

2.2.2 Grey-box approaches

A particular advantage of models obtained using grey-box techniques is that they can be tailored to reproduce specific relevant features and/or to meet possible constraints on the structure and parameters to make them suitable for model-based control or compensation schemes (Pearson, 1999; Aguirre, 2019). Although the use of specific hysteresis-motivated regressors $\phi_{i,k}$ is beneficial, some works apparently adopted them without a specific justification (Leva and Piroddi, 2002; Worden and Barthorpe, 2012; Lacerda Júnior et al., 2019). In this sense, such works build models following a weakly – or dark – grey-box approach. ‘Clearer’ grey-box techniques include specific regressors based on auxiliary information or some kind of prior knowledge such as physical insights about dynamic and/or static behaviour of the investigated system.

Given both directions covered above, i.e., the black-box and weakly grey-box approaches, we will now revisit in more detail three works that take a different look at

enabling NARX polynomials to deal with some subtle aspects of hysteresis nonlinearity.

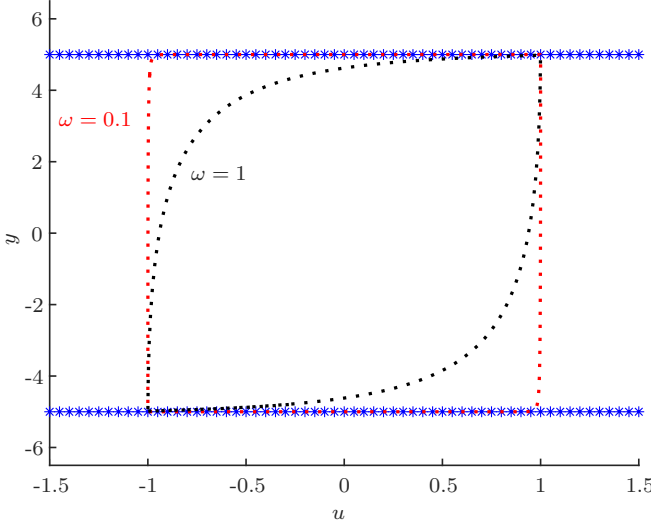
As far as we know and as stated by Deng and Tan (2009), their work is probably the first in the literature on grey-box modelling of hysteretic systems using NARX polynomials, where specific actions to capture the basic behaviour or the change tendency of the hysteresis nonlinearity were made. A key point of this work was the proposal of a hysteretic operator to be used as an additional regressor $\phi_{i,k}$ of a NARX model (12). The following hysteretic operator was proposed (Deng and Tan, 2009):

$$h_k \triangleq h(u_k) = |\arctan(u_k - u_{ext,k})| [u_k - u_{ext,k}] + h(u_{ext,k}), \quad (15)$$

where $h_k \in \mathbb{R}$ is the output of the operator, $u_k \in \mathbb{R}$ is the current input, $u_{ext,k}$ refers to the dominant extremum adjacent to u_k , and $h(u_{ext,k})$ is the output of the operator when the input is $u_{ext,k}$. Both $u_{ext,k}$ and $h(u_{ext,k})$ can be initialised to null values. See Deng and Tan (2009), Deng et al. (2014) and Tan and Deng (2014) for more details.

Deng and Tan (2009) showed that the hysteretic operator (15) is able to describe some subtle features found in hysteretic systems, such as the ascending, turning and descending behaviour that give rise to the hysteresis loop displayed on the input-output plane when such systems are subjected to time-varying input signals. In a similar vein, some interesting discussions on the action of adding new inputs $\phi_{i,k}$ to the model have been addressed by Mohammadzaheri et al. (2012) in order to transform the hysteresis multi-valued mapping into a one-to-one mapping so that NARX models can be employed to describe the hysteresis behaviour.

Figure 5 The black and red dots are on $\mathcal{H}_k(\omega)$ for model (16) (see online version for colours)



Notes: The bounding structure \mathcal{H} (17) in blue (*) will always confine $\mathcal{H}_k(\omega)$. The top limit corresponds to a loading situation, whereas the bottom limit, to unloading.

Martins and Aguirre (2016) proposed sufficient conditions for NARX polynomial models to be able to display a loop

when subject to low-frequency loading-unloading input signals. Key features were the explicit use of equilibria, of multi-valued functions adopted as a candidate regressor $\phi_{i,k}$ of a model (12), such as the sign function, and the definition of a bounding structure \mathcal{H} that serves as a boundary for the loop.

Example 2.1: Consider the following autoregressive model (Martins and Aguirre, 2016):

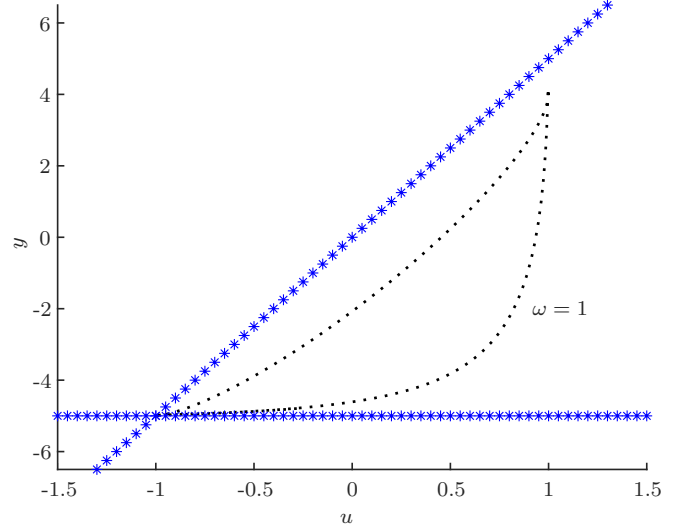
$$y_k = c_y(1)y_{k-1} + c_{\phi_2}(1)\phi_{2,k-1}, \quad (16)$$

for which $c_y(1) = 0.9$, $c_{\phi_2}(1) = 0.5$, $\phi_{2,k} = \text{sign}(\phi_{1,k})$, $\phi_{1,k} = u_k - u_{k-1}$, and $u_k = \sin(\omega k)$, whose term clusters Ω_y has coefficient $\Sigma_y = c_y(1) = 0.9$ and Ω_{ϕ_2} with $\Sigma_{\phi_2} = c_{\phi_2}(1) = 0.5$ [Abreu, (2021), Definition 2.2] respectively, and the sampling time is set to $T_s = 0.05$ s. The equilibria are given by:

$$\bar{y}(\phi_2) \approx \begin{cases} \frac{\Sigma_{\phi_2}}{1 - \Sigma_y} = 5, & \text{for } \bar{\phi}_2 = 1 \text{(loading);} \\ \frac{-\Sigma_{\phi_2}}{1 - \Sigma_y} = -5, & \text{for } \bar{\phi}_2 = -1 \text{(unloading)}, \end{cases} \quad (17)$$

which form the bounding structure that confines the loop (see Figure 5). The input frequency influences the shape of the loop $\mathcal{H}_k(\omega)$ but not the bounding structure \mathcal{H} .

Figure 6 The black dots are on $\mathcal{H}_k(\omega)$ for model (16) with regressor (18) (see online version for colours)



Notes: The bounding structure \mathcal{H} in blue (*) will always confine $\mathcal{H}_k(\omega)$.

The next example shows how to produce an asymmetrical loop using a NARX model.

Example 2.2: For model (16) in Example 2.1, it is assumed that the regressor $\phi_{2,k} = \text{sign}(\phi_{1,k})$ with $\phi_{1,k} = u_k - u_{k-1}$, which is symmetric, is replaced by an asymmetric multi-valued function, given by (Martins, 2016):

$$\phi_{2,k} = \begin{cases} u_k, & \text{if } \phi_{1,k} > 0; \\ -1, & \text{if } \phi_{1,k} < 0; \\ 0, & \text{if } \phi_{1,k} = 0. \end{cases} \quad (18)$$

For $\omega = 1$, \mathcal{H} and $\mathcal{H}_k(\omega)$ are shown in Figure 6.

The conditions proposed by Martins and Aguirre (2016) do not guarantee the existence of multiple fixed points at steady-state, which is an important feature for hysteretic systems (Bernstein, 2007; Morris, 2011). Conditions for this will be provided in the following.

The persistent loop behaviour exhibited in the input-output plane (e.g., see Figure 5) has been widely accepted as the hallmark of hysteretic systems. Hence, many papers were devoted to model hysteretic systems focused only on the description of their hysteresis loop or time response (Ni et al., 1998; Smyth et al., 2002; Hu and Ben Mrad, 2003; Oh and Bernstein, 2005; Al Janaideh et al., 2008; Zakerzadeh et al., 2011; Domínguez-González et al., 2014; Zhang et al., 2017a). Fundamental questions arise: *does this feature suffice to assess whether an identified hysteretic model is really representative? or rather, what is hysteresis?*

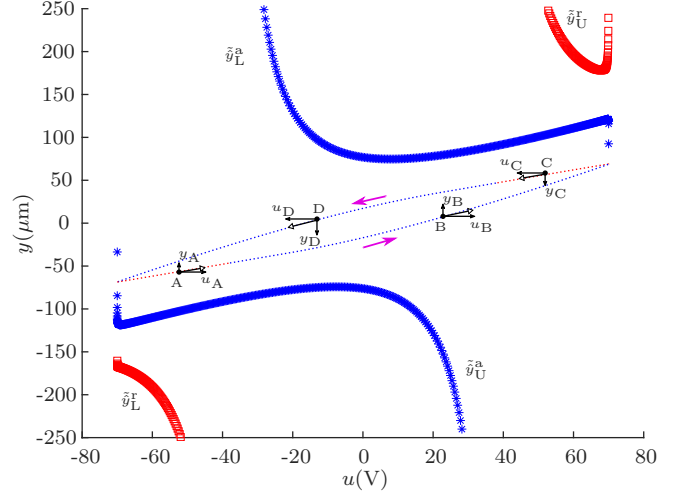
Faced with the last question, Bernstein (2007) and Morris (2011) provided a detailed discussion that goes far beyond the simple fact that hysteretic systems have a characteristic loop and analysed what causes it in different contexts. Based on such valuable insight, Abreu et al. (2020) defined, in addition to the hysteresis loop, a *continuum of steady-state solutions* as an important feature that is expected in steady-state. Structure and parameter constraints were proposed to guarantee such a feature in the identified models. A more general framework, based on a *quasi-static analysis*, was developed to explain how the hysteresis loop occurs in such models as an interplay of *attracting* and *repelling regions/points* in the input-output plane. As pointed out in Abreu (2021), the authors are not aware of any studies that impose this feature during the identification procedure or that show the performance of the identified NARX models for constant inputs, e.g., see Leva and Piroddi (2002), Parlitz et al. (2004), Worden et al. (2007), Deng and Tan (2009), Worden and Barthorpe (2012), Martins and Aguirre (2016), Zhang et al. (2017a) and Lacerda Júnior et al. (2019).

Example 2.3: Consider the NARX model of a simulated PEA (Abreu, 2021):

$$\begin{aligned} \hat{y}_k &= \hat{\theta}_1 \hat{y}_{k-1} + \hat{\theta}_2 \phi_{1,k-2} + \hat{\theta}_3 \phi_{2,k-2} \phi_{1,k-2} u_{k-2} \\ &+ \hat{\theta}_4 \phi_{2,k-2} \phi_{1,k-2} \hat{y}_{k-1} + \hat{\theta}_5 \phi_{1,k-2} u_{k-2}^2 \\ &+ \hat{\theta}_6 \phi_{1,k-2} u_{k-2} \hat{y}_{k-1} + \hat{\theta}_7 \phi_{2,k-2} \hat{y}_{k-1} \\ &+ \hat{\theta}_8 \phi_{1,k-1} + \hat{\theta}_9 \phi_{2,k-2} \phi_{1,k-2}^2, \end{aligned} \quad (19)$$

with $\hat{\theta}_1 = 1.0000$, $\hat{\theta}_2 = -0.2310$, $\hat{\theta}_3 = 0.0146$, $\hat{\theta}_4 = -0.0099$, $\hat{\theta}_5 = 3.2333 \times 10^{-4}$, $\hat{\theta}_6 = -2.5494 \times 10^{-4}$, $\hat{\theta}_7 = 1.7891 \times 10^{-5}$, $\hat{\theta}_8 = 1.0080$, $\hat{\theta}_9 = -0.0604$, $\phi_{2,k} = \text{sign}(\phi_{1,k})$, $\phi_{1,k} = u_k - u_{k-1}$, u_k is the voltage input, and y_k is the position output. Model (19) complies with the constraints proposed in Abreu et al. (2020). Steady-state analysis is done by taking $\hat{y}_k = \bar{y}, \forall k$, $u_k = \bar{u}, \forall k$ and, consequently, $\phi_{1,k} = u_k - u_{k-1} = 0$ and $\phi_{2,k} = \text{sign}(\phi_{1,k}) = 0, \forall k$, this yields: $\bar{y} = \hat{\theta}_1 \bar{y}$ with $\hat{\theta}_1$ constrained to be 1, as required by Abreu (2021).

Figure 7 Results of quasi-static analysis for model (19) with input $u_k = 70\sin(2\pi k)V$ and a sampling time of $T_s = 0.001$ s (see online version for colours)



Notes: The hysteresis loop indicated with (...) is a result of the interaction of (*) attracting (\hat{y}_L^a , \hat{y}_U^a) and (□) repelling (\hat{y}_L^r , \hat{y}_U^r) points/sets. (→) indicates the orientation of the hysteresis loop. (●) refers to specific output values under loading, in A and B, and unloading, in C and D.

The quasi-static analysis of model (19) yields:

$$\begin{aligned} \tilde{y}_k &\approx \hat{\theta}_1 \tilde{y}_k + \hat{\theta}_2 \phi_{1,k-2} + \hat{\theta}_3 \phi_{2,k-2} \phi_{1,k-2} u_{k-2} \\ &+ \hat{\theta}_4 \phi_{2,k-2} \phi_{1,k-2} \tilde{y}_k + \hat{\theta}_5 \phi_{1,k-2} u_{k-2}^2 \\ &+ \hat{\theta}_6 \phi_{1,k-2} u_{k-2} \tilde{y}_k + \hat{\theta}_7 \phi_{2,k-2} \tilde{y}_k + \hat{\theta}_8 \phi_{1,k-1} \\ &+ \hat{\theta}_9 \phi_{2,k-2} \phi_{1,k-2}^2, \end{aligned}$$

which gives:

$$\tilde{y} \approx \begin{cases} \frac{\hat{\theta}_2 \phi_1 + \hat{\theta}_3 \phi_1 u + \hat{\theta}_5 \phi_1 u^2 + \hat{\theta}_8 \phi_1 + \hat{\theta}_9 \phi_1^2}{1 - \hat{\theta}_1 - \hat{\theta}_4 \phi_1 - \hat{\theta}_6 \phi_1 u - \hat{\theta}_7}, & \text{for } \phi_2 = 1; \\ \frac{\hat{\theta}_2 \phi_1 - \hat{\theta}_3 \phi_1 u + \hat{\theta}_5 \phi_1 u^2 + \hat{\theta}_8 \phi_1 - \hat{\theta}_9 \phi_1^2}{1 - \hat{\theta}_1 + \hat{\theta}_4 \phi_1 - \hat{\theta}_6 \phi_1 u + \hat{\theta}_7}, & \text{for } \phi_2 = -1, \end{cases} \quad (20)$$

where the time indices have been omitted for clarity, and whose solution \tilde{y}_k is in an attractive region/point if the following condition is satisfied:

$$\begin{aligned} -1 &< \hat{\theta}_1 + \hat{\theta}_4 \phi_{2,k-2} \phi_{1,k-2} + \hat{\theta}_6 \phi_{1,k-2} u_{k-2} \\ &+ \hat{\theta}_7 \phi_{2,k-2} < 1, \frac{-1 - \hat{\theta}_1 - \hat{\theta}_4 \phi_{2,k-2} \phi_{1,k-2} - \hat{\theta}_7 \phi_{2,k-2}}{\hat{\theta}_6 \phi_{1,k-2}} \\ &< u_{k-2} < \frac{1 - \hat{\theta}_1 - \hat{\theta}_4 \phi_{2,k-2} \phi_{1,k-2} - \hat{\theta}_7 \phi_{2,k-2}}{\hat{\theta}_6 \phi_{1,k-2}}. \end{aligned} \quad (21)$$

The solutions of equation (20) are computed and using equation (21) one verifies whether they belong to attracting or repelling sets under loading, represented by \hat{y}_L^a and \hat{y}_L^r , or unloading, by \hat{y}_U^a and \hat{y}_U^r . If a solution \hat{y}_k belongs to an attractive region \hat{y}^a , then the model output \hat{y}_k has

a component in that direction and is pulled towards the attracting set. The other component is due to loading or unloading. This interplay between attractive or repulsive regions/points with a loading-unloading input signal is illustrated in Figure 7 and helps to explain how the hysteresis loop is formed.

For details on the need for constraints see Abreu et al. (2020), Abreu (2021) and Tavares et al. (2021, 2022).

2.3 Topics for future work

A number of features and properties related to hysteresis are still subject to study. Thus, in this section, we point out some interesting properties of hysteretic systems and briefly suggest alternative ways to achieve them using grey-box NARX models.

According to Mayergoyz (2003), *non-local memory* is a property found in some hysteretic systems in which the future value of the output depends not only on the current value of the output and input, but also on past extremum values of the input. Thus, a striking feature of such systems is the existence of more than one distinct trajectory for any reachable state in the input-output plane, and which one the state will follow depends on a particular sequence of past extremum values of input (de Almeida et al., 2003; Merola et al., 2015). In addition, some works in the literature also associate non-local memory with the existence of crossing and partially coincident *minor loops* (Mayergoyz, 2003; Berenyi et al., 2005; Drincic and Bernstein, 2009; Liu and Yang, 2015; Jankowski et al., 2017). Conversely, hysteretic systems with *local memory* have their future output value dependent only on the current output and input value, without being influenced by past extremum values. For this type of hysteresis, a common feature is that for any reachable state in the input-output plane, its next values will be reached through only one trajectory for increasing the input and one for decreasing it.

Some have stated that there is a lack of evidence for non-local memory, while others for local memory (Mayergoyz, 2003; de Almeida et al., 2003). For instance, considering the phenomenological models (Subsection 2.1), those based on differential equations, such as the Bouc-Wen model, the Duhem model, the Dahl and the LuGre model, have commonly been related to hysteresis with local memory, while those based on operators, such as the Preisach and the Prandtl-Ishlinskii models, have been shown to be able to capture the property of non-local memory.

In the case of hysteretic systems with non-local memory, it is essential that the models used to describe these systems incorporate in their structure ways to detect and store input extremum values, such as the Preisach model (Ge and Jouaneh, 1996; Al-Bender et al., 2004). The use of extremum values of the input in the proposed hysteretic operator (15) might be a promising way to indirectly incorporate non-local memory in NARX models. A key question is: *what are the true benefits in terms of predictive and compensation performance if the model had*

non-local memory? See Swevers et al. (2000), Bashash and Jalili (2006) and Liu and Yang (2015) for some related discussions.

The symmetry of the hysteresis loop is usually attributed to the type of material used: piezoceramic actuators are known to generally produce symmetric hysteresis loops (Yu et al., 2002; Cao et al., 2019), whereas shape memory alloys and magnetostrictive actuators tend to have asymmetric loops (Kuhnen, 2003; Shakiba et al., 2018). The models reviewed in Subsection 2.1 were developed to describe symmetric hysteresis, however, many works have proposed ways to incorporate asymmetric hysteresis into such classical phenomenological models (Ge and Jouaneh, 1995; Gu et al., 2014; Wei et al., 2014). In terms of NARX models, the works reviewed in Subsection 2.2.2 identify models that tend to reproduce symmetric hysteresis loops (e.g., see Figure 5), but it is also possible to produce asymmetrical loops, as illustrated in Example 2.2 with the use of an asymmetric multi-valued function. However, there are some relevant questions that have not yet been answered and require further investigation. In short, two fundamental questions arise: *how to determine an appropriate asymmetric multi-valued function to be used?* and *how will this function affect the number, location, and stability of the fixed points?* Indeed, the systematic shaping of asymmetric loops is an open topic for research.

3 Tools for NARX models identification

In this section, some tools for *black-box* and *grey-box* identification of NARX polynomial models (11) are presented. The MGGP approach for identifying a system with hysteresis is also introduced.

For the sake of simplicity, consider a *single-input single-output* (SISO) system \mathcal{S} , from where a series of measured N input-output pairs are available, $\{y_k, u_k\}$ for $k = 1, \dots, N$, where k is the discrete time index. If equation (12) is intended, the additional regressors $\phi_{i,k}$ can be readily computed from the measurements. Considering the measured data $Z = [yu] \in \mathbb{R}^{N \times 2}$, the objective of system identification is to find a model \mathcal{M} that in some sense behaves like \mathcal{S} (Aguirre et al., 2010).

To find \mathcal{M} , the identification problem can be written as the optimisation problem:

$$\underset{\hat{\theta}, \psi}{\text{minimise}} \quad J(\mathbf{y}, \hat{\mathbf{y}}), \quad (22)$$

where $\hat{\mathbf{y}}$ is the model output, $\hat{\theta} \triangleq [\hat{\theta}_1, \dots, \hat{\theta}_{n_\theta}]^T \in \mathbb{R}^{n_\theta}$ is the estimated parameter vector with n_θ as the number of terms in the model \mathcal{M} , and $\psi_{k-1} \triangleq [\psi_1, \dots, \psi_{n_\theta}]^T \in \mathbb{R}^{n_\theta}$ is the regressor vector composed of linear and nonlinear combinations of output $y_{k-1}, \dots, y_{k-n_y}$, input $u_{k-\tau_d}, \dots, u_{k-n_u}$ and, optionally, additional terms $\phi_{i,k-1}, \dots, \phi_{i,k-n_{\phi_i}}$. Thus, the identification problem can be decomposed into two subtasks, namely *structure selection* and *parameter estimation*.

Because NARX polynomial models are linear-in-the-parameters the output \hat{y} can be written as:

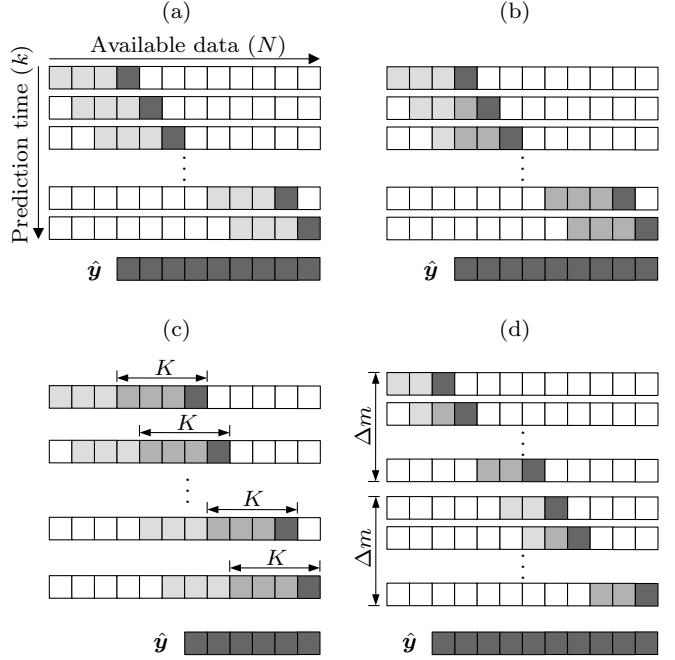
$$\hat{y}_k = \psi_{k-1}^T \hat{\theta} = \sum_{l=1}^{n_\theta} \hat{\theta}_l \psi_{l,k-1}. \quad (23)$$

Model (23) can be promptly used in the aforementioned optimisation problem. However, there are many ways of producing \hat{y}_k by simulation as illustrated in Figure 8. Each type of simulation yields a different problem with different features.

- *One-step-ahead prediction*: $\hat{y} = \Psi \hat{\theta}$ are obtained using the available information up to and including step $k-1$, where $\Psi \triangleq [\psi_1 \psi_2 \dots \psi_{n_\theta}] \in \mathbb{R}^{N \times n_\theta}$ is the regressor matrix composed by measured data. The methods that apply this simulation in equation (22) are called *prediction error minimisation* (PEM) approaches. As a general rule, one-step-ahead predictions are not good indicators of the model capability to explain system dynamics (Piroddi, 2008; Aguirre et al., 2010; Barbosa et al., 2011). Figure 8(a) shows a graphical representation of this method, where each column represents a time index of the measured data and each row represents a time index of the model predictions. For the *one-step-ahead* prediction, all initial conditions used for model simulation are from measured data.
- *Free-run prediction*: $\hat{y}_k = \hat{\psi}_{k-1}^T \hat{\theta}$ is a recursive simulation that predicts infinite steps ahead using the input and previously predicted output values, this is indicated by the hat on $\hat{\psi}_{k-1}^T$ and in Figure 8(b) by the medium grey squares. Identification techniques based on this simulation methods are called *simulation error minimisation* (SEM) approaches. This criterion may be seen as dynamically more representative than the previous PEM approach, as discussed in Piroddi and Spinelli (2003), Piroddi (2008), Aguirre et al. (2010), Barbosa et al. (2011) and Ribeiro et al. (2020).
- *Multi-step-ahead prediction*: In this case, the free-run simulation is truncated to K steps ahead and reset soon after with a one-step moving horizon. The K -step-ahead PEM (KSA) approach implemented uses this type of simulation. Figure 8(c) represents the multi-step-ahead prediction setting. A free-run simulation is performed during K steps and the last estimated value is taken as the prediction output. The process is reset at each prediction time.
- *Multiple shooting (MS)*: The data are split into M intervals of size Δm , each with its own initial condition y_0^j , for $j = 1, \dots, M$. A free-run simulation is performed on each interval. This yields MS identification approaches that allow optimisation problems to be solved that would be computationally infeasible in a free-run simulation setting. Besides, according to Ribeiro et al. (2020), since the simulation is limited to a shorter interval, Δm , the

objective function (22) becomes smoother, helping the optimisation procedure to find better solutions. In Figure 8(d), the prediction horizon is divided into two intervals of size Δm and an independent free-run simulation is performed for each of them.

Figure 8 Simulation methods, light grey (■) represents original data used as initial conditions, medium grey (■) represents predicted data used as initial conditions and dark grey (■) represents the model's output (\hat{y}_k), (a) one-step-ahead prediction (b) free-run simulation (c) multi-step-ahead prediction (d) MS



3.1 Structure selection

NARX polynomial models suffer from the well known curse of dimensionality, i.e., the number of terms (regressors in ψ_{k-1}) grows rapidly with n_y , n_u , n_{ϕ_i} and ℓ . The problem of model structure selection is to find a proper set of terms.

In this case, for a SISO system, considering m as the number of possible linear terms in equation (12) ($m = n_y + n_u - \tau_d + n_{\phi_i}$), the total number of possible polynomial terms, and consequently of model parameters, is given by (Madár et al., 2005):

$$n_\theta = \frac{(\ell + m)!}{\ell! m!}, \quad (24)$$

which yields a huge total number of possible different models (2^{n_θ}), transforming the structure selection task into a combinatorial optimisation problem.

One of the most used criteria for structure selection for NARX models is the *error reduction ratio* (ERR) (Billings and Chen, 1989b). It evaluates the relevance of a regressor candidate regarding its capacity to explain the output variance. For instance, in the *forward regression orthogonal estimator* (FROE) algorithm (Billings et al.,

1989) the model structure is incremented iteratively until a certain precision of one-step-ahead prediction is achieved. In FROE, the model parameters are estimated via the *orthogonal least squares* (OLS) method. These orthogonalisation techniques are designed in such a way that, at each step, the relevance of each regressor candidate can be assessed separately via the ERR:

$$[ERR]_l = \frac{\hat{g}_l^2 \sum_{k=1}^N w_{l,k}^2}{\sum_{k=1}^N y_k^2}, \quad (25)$$

where w_l is the l^{th} auxiliary orthogonal regressor and \hat{g}_l is its corresponding estimated parameter (Billings, 2013). Regressors with higher ERR are included in the model. Some similar techniques are proposed in the literature to accomplish structure selection and parameter estimation at the same time (Chen et al., 1989; Wei and Billings, 2008).

Piroddi and Spinelli (2003) pointed out some limitations of PEM methods, such as the ERR. It is shown that, in the presence of certain characteristics of noise or of input signals, these methods may find incorrect or redundant models. In such cases, they are considered local search techniques with a great probability of finding sub-optimal solutions, and models can be extremely imprecise and even unstable.

Thus, to circumvent such limitations, Piroddi and Spinelli (2003) proposed to replace the ERR criterion by the *simulation error reduction ratio* (SRR) criterion, which is defined by the reduction of the *mean squared simulation error* (MSSE) normalised by the variance of the system output signal:

$$[SRR]_l = \frac{MSSE(\mathcal{M}_l) - MSSE(\mathcal{M}_{l+1})}{\frac{1}{N} \sum_{k=1}^N y_k^2} \quad (26)$$

where \mathcal{M}_l is the model structure in the l^{th} iteration and \mathcal{M}_{l+1} is the candidate model for the subsequent iteration with the inclusion of the $l+1^{\text{th}}$ regressor. Hence the model structure selection operation is performed based on the minimisation of the simulation error (SEM approach). Although SEM approaches normally perform better in certain conditions, they demand higher computational processing.

In Falsone et al. (2015), an iterative *randomised algorithm for model structure selection* (RaMSS) was proposed focusing on NARX models, where PEM and SEM approaches were tested and also combined. It was shown that the use of simulation error increases the ability of the algorithm to discard models that have apparently a good performance, but that do not represent well the underlying dynamics of the system. Related works include (Bianchi et al., 2016, 2021; Fagundes et al., 2022).

Most of the solutions for structure selection in the literature, from the classic FROE to the probabilistic approaches like RaMSS and those based on metaheuristics as presented in Hafiz et al. (2020a), build a pool of candidate terms which can become very large. To avoid this, the use of methods where the creation and selection of the regressors are performed concomitantly can be used. This will be explored here using the MGGP algorithm.

An interesting though largely unexploited problem is that of quantifying the uncertainty related to model structure for nonlinear systems. Some preliminary studies are Barbosa et al. (2015) and Gu and Wei (2018).

3.2 Parameter estimation

The parameters of a linear-in-parameters model can be estimated via the *least squares* (LS) estimator (Ljung, 1999):

$$\hat{\theta}_{LS} = (\Psi^T \Psi)^{-1} \Psi^T \mathbf{y}. \quad (27)$$

If the parameters are related to a linear set of equality constraints in the form $\mathbf{c} = S\theta$, where $\mathbf{c} \in \mathbb{R}^{n_c}$ and $S \in \mathbb{R}^{n_c \times n_\theta}$ are known constants, parameters can be obtained using the *constrained least squares* (CLS) estimator (Draper and Smith, 1998):

$$\begin{aligned} \hat{\theta}_{CLS} = \\ \hat{\theta}_{LS} - (\Psi^T \Psi)^{-1} S^T [S(\Psi^T \Psi)^{-1} S^T]^{-1} (S\hat{\theta}_{LS} - \mathbf{c}), \end{aligned} \quad (28)$$

where Ψ is the regressor matrix and $\hat{\theta}_{LS}$ is the solution of equation (27). Such an algorithm is useful for estimating the parameters in a grey-box setting (Aguirre, 2019).

Another way of using auxiliary information during parameter estimation is via multi-objective optimisation (Barroso et al., 2007; Nepomuceno et al., 2007; Hafiz et al., 2020b, 2020a; Freitas et al., 2021).

Next, we introduce the core idea of *evolutionary algorithms* (EAs) and some particular categories of such algorithms in applications for systems identification.

3.3 Evolutionary algorithms

EAs comprise a set of metaheuristics based on metaphors of natural/biological processes used to build computational models capable of solving problems. There is a wide variety of proposed algorithms that simulate the evolution of species through natural phenomena of selection, mutation, and reproduction that occur in a given population of individuals. Generally, an EA has a standard behaviour: it begins with an initial population of random individuals (chromosomes) and at each generation (main loop) the best solutions are sought (*selection*), then combined (*recombination/reproduction/crossover* and *mutation*) in order to generate even better solutions. There are two features that differ one EA from another:

- 1 the genetic representation
- 2 the evolution process.

The genetic representation is concerned with how the solutions are codified for a proper computer simulation. There are several ways to represent a solution and their choice depends on the problem being solved. For instance, if the problem is the structure selection of NARX polynomial models, one may represent the solutions as a

binary string in which each bit represents one candidate term (Chen et al., 2007; Hafiz et al., 2020a). Terms with ‘true’ value are included in the model. If the problem is parameters estimation, one may use a vector of real numbers as representation, such that each *locus* is an estimated parameter (Aguirre et al., 2010; Barbosa et al., 2011).

Evolution processes are characterised by parent selection and recombination/mutation methods. These methods depend on the implemented genetic representation that can be classified into two groups:

- 1 *chromosome-based*
- 2 *tree-based* representations.

A *chromosome-based* representation consists of a vector of values where each index (*locus*), or a set of indexes (*gene*), corresponds to a specific feature of the solution. In the *tree-based* representation, from a root node, the tree is divided into several branches in which the internal nodes are composed of arithmetic functions (+, −, ×, ÷, max, ...) and the terminals, also called leaves, are composed of variables and constants. As a result, this representation hierarchically synthesises a mathematical function, thus, not requiring the user to specify the structure of the solution *a priori*.

The concept of *fitness* is of great importance for these algorithms. One must define an evaluation function (or cost function) that assigns a quality measure to each individual (possible solution). This *fitness* is the basis for selecting the best individuals from a population and it is the direct link of the algorithm to the real problem.

In what follows, we present three different EAs, namely *genetic algorithms* (GAs) (Goldberg and Holland, 1988), *genetic programming* (GP) (Koza, 1994) and *MGGP* (Hinchliffe and Willis, 2003), and some applications in system identification.

3.3.1 Genetic algorithms

GAs are *chromosome-based* EAs. The representation of the solutions may be a binary string, a vector of real values or a mix of those. The definition of the *genes* representation in a *chromosome* depends on the problem being solved. Goldberg and Holland (1988) define the classic GA with a *binary* representation, *roulette wheel* selection and *one-point crossover* reproduction. Figure 9 presents two genetic operators for a binary *chromosome-based* representation:

- a *one-point crossover*
- b *uniform mutation*.

In the former, a cutoff point is selected and the parent individuals exchange genetic material by concatenating the left part of one parent with the right of the other and vice-versa. In the latter, each *locus* has an independent probability of flipping its value (0 → 1 or 1 → 0).

Regarding real representations, different *crossover* operators can be used. For instance, in the *flat crossover* operator (Radcliffe, 1991), the value of the gene *i* in the offspring chromosome *h* is chosen randomly from the interval $[c_i^1, c_i^2]$, where c_i^j is the gene *i* of the parent chromosome *j*; in the *arithmetical crossover* operator, the offspring chromosomes h^1 and h^2 are generated according to the relationships $h_i^1 = \lambda c_i^1 + (1 - \lambda)c_i^2$ and $h_i^2 = \lambda c_i^2 + (1 - \lambda)c_i^1$, where λ is chosen from the interval [0, 1] and may vary over generations (Eiben and Smith, 2015); and in the *BLX - α crossover* operator, also called *blend crossover*, the offspring h_i is chosen randomly in the interval $[c_{\min} - I\alpha, c_{\max} + I\alpha]$, where $c_{\max} = \max(c_i^1, c_i^2)$, $c_{\min} = \min(c_i^1, c_i^2)$ and $I = c_{\max} - c_{\min}$; see more at Herrera et al. (1998).

Figure 9 Examples of crossover and mutation operators for a binary *chromosome-based* representation,
(a) one-point crossover (b) uniform mutation

		Cutoff Point		
Parent 1	0 1 1		Individual	0 1 1 0 0 1 0 1
Parent 2	1 0 0		Mutated	0 0 1 0 1 1 0 1
Offspring 1	1 0 0		Individual	0 0 1 0 1 1 0 1
Offspring 2	0 1 1			

Li and Jeon (1993) developed a GA-based system identification method to automatically construct NARX polynomial models. Their method is used to identify three simulated examples, a simulated NARX system corrupted with noise, the Mackey-Glass equation and the Van der Pol oscillator. The binary representation is employed and each *locus* represents a candidate model term.

Chen et al. (2007) employed the GA to identify the coefficients and the structure of ARX models basing on the prediction error and correlation functions between the model residuals and the input/output signals. Each solution (or chromosome) is defined as a binary string. To fit all the parameters of an ARX model, the binary string of a solution is divided into some sub-strings, which are called *genes*, and each *gene* is translated into a parameter of the ARX model.

Ali et al. (2021) compared the performance of the GA with the *particle swarm optimisation* (PSO) and *cuckoo search* (CS) algorithms when used to estimate the parameters of a photovoltaic model. A theoretical analysis to prove the convergence of the CS algorithm can be found in Sun et al. (2021).

A multi-objective EA approach to identify NARX polynomial models was implemented in Aguirre et al. (2010) to compare PEM and SEM parameter estimation. Barbosa et al. (2011) implemented the GA to estimate parameters of NARX models of a pilot hydraulic pumping system using a bi-objective optimisation approach to minimise the simulation error and the model static curve error (*grey-box* identification). A GA-based NARX model identification for evaluation of insulin sensitivity can be

seen in Ghosh and Maka (2011). Hafiz et al. (2020b) proposed a *grey-box* identification approach to model a pilot DC-DC buck converter using a multi-objective framework for structure selection using string-based chromosomes. Barbosa et al. (2019) applied GA to identify the submodels partitions of PieceWise ARX models (PWARX). Inputs for NARX neural models were selected by EAs in de Moraes et al. (2019) to design soft sensors for a petrochemical process. Finally, Le Guisquet and Amabili (2021a, 2021b) estimated the nonlinear damping and stiffness parameters of harmonically forced continuous systems by means of GA.

3.3.2 Genetic programming

The *tree-based* representation forms the basis for a branch of EAs known as GP. In this algorithm, the structure of the solution is not specified in advance and the individuals are computer programs that randomly evolve into new programs. The problem consists of building a function or a program that makes the mapping between input and output data. Individual performance is assessed by running the program and determining its error related to the desired output. In this representation, from a root node, the tree is divided into several branches that hierarchically synthesise a mathematical function. Figure 10 presents two genetic operators for a *tree-based* representation:

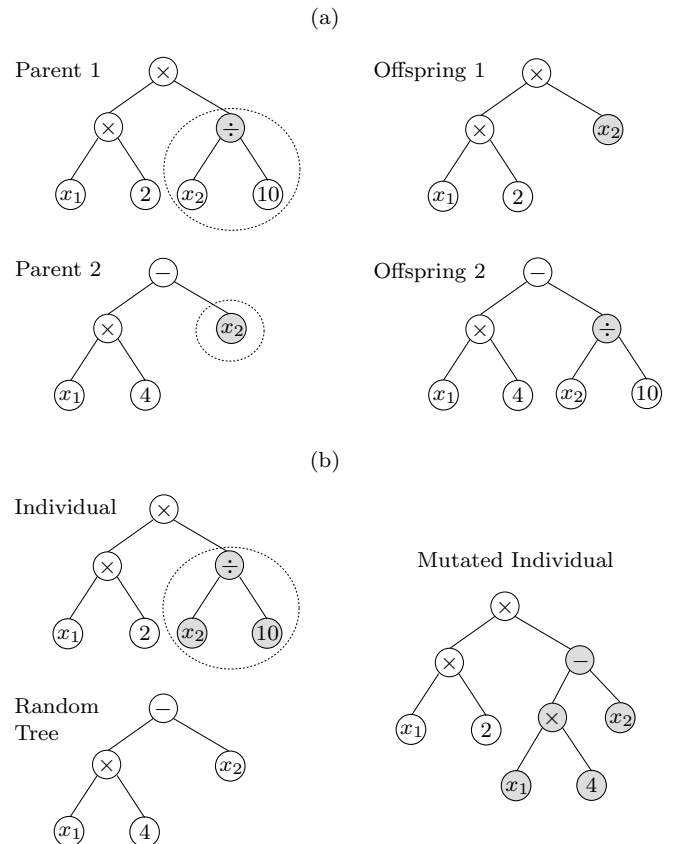
- a subtree crossover
- b subtree mutation.

In the former, a node is selected at random for each parent and the subtrees formed from these root nodes are exchanged as genetic materials. Then, from the parents $p_1(x_1, x_2) = 2x_1 \frac{x_2}{10}$ and $p_2(x_1, x_2) = 4x_1 - x_2$ it is constructed the offsprings $o_1(x_1, x_2) = 2x_1 x_2$ and $o_2(x_1, x_2) = 4x_1 - \frac{x_2}{10}$. In the latter, a node is selected at random and the subtree formed from this root node is replaced by a new randomly generated subtree. Then, the individual $p_1 = 2x_1 \frac{x_2}{10}$ is mutated into $p_m(x_1, x_2) = 2x_1(4x_1 - x_2)$. For more details on GP and its genetic operators see Poli et al. (2008).

Rodriguez-Vazquez et al. (2004) described a *multi-objective GP* (MOGP) optimisation approach employed to identify NARMAX model structures for a gas turbine engine. The incorporation of a multi-objective approach allowed the implementation of objectives related to model complexity and model performance. A key advantage of the MOGP method is to provide a family of potential models that address issues concerning the complexity, flexibility, and validity of a model. Madár et al. (2005) proposed a hybridisation of GP and the OLS method for the structure selection of NARX models. Thus the regressors that are less significant (low ERR) are removed from the model. This pruning method is applied before the evaluation step. Khandelwal et al. (2019a, 2019b) proposed a representation that uses *tree adjoining grammar* (TAG) (Joshi, 1987; Joshi and Schabes, 1997; Kallmeyer, 2009). The use of TAG allows the representation of dynamical

models in terms of a set of fundamental building blocks called *elementary trees*. The advantage of TAG-based representations is the use of a set of elementary trees to generate models that belong to different classes of dynamical systems, making the combinatorial search more efficient by restricting the search space explored by GP.

Figure 10 Examples of crossover and mutation operators for *tree-based* representation, (a) subtree crossover
(b) subtree mutation



3.3.3 Multi-gene genetic programming

A mixed *chromosome/tree-based* representation was proposed by Hinchliffe and Willis (2003) as the basis of the MGGP algorithm. MGGP also uses weighted sum of basis functions $g_i(\varphi)$ of output and input signals:

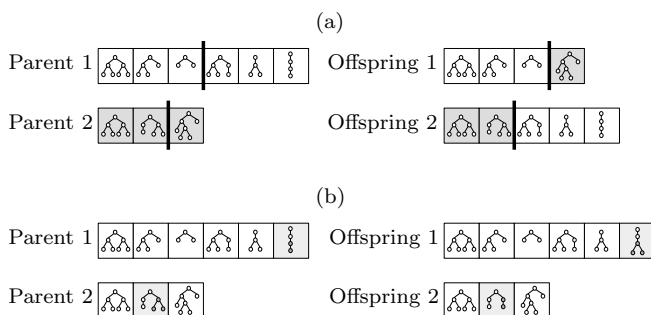
$$g(\varphi, \theta) = \sum_{i=1}^m \theta_i g_i(\varphi). \quad (29)$$

In this sense, an MGGP individual consists of a vector (*chromosome*) of *tree-based* programs (GP) as basis functions. A solution is a linear combination of the outputs of a set of GP individuals. Such structure fits naturally in the NARX context, since each tree (or GP individual) may correspond to one model term. Model (29) should be compared to equation (23).

The main difference between the MGGP genetic operators and those of the standard GP is the recombination operators. In MGGP, they are referred to as *high-level crossover* and *low-level crossover*. In the former, the genetic

materials are exchanged as entire basis functions; that is, the MGGP parents exchange their GP individual in a way similar to GA one-point crossover. However, notice that in *high-level crossover*, the resultant offsprings can have different sizes from each other and even from their parents. This occurs because a different cutoff point is chosen for each parent. Hence, the MGGP algorithm works with fluctuating individual sizes. In the *low-level crossover*, the genetic materials are exchanged as subtrees of the basis functions; that is, only one gene is randomly chosen from each parent individual, and their GPs (or basis functions) exchange genetic materials as in the GP *subtree crossover operator*. Figure 11 illustrates these operators.

Figure 11 Examples of crossover operators for the mixed chromosome/tree-based representation, (a) high-level crossover (b) low-level crossover



The MGGP was used to build dynamical models for an industrial cooking extruder (Hinchliffe and Willis, 2003). The appropriate lag terms required to build an accurate model are chosen automatically. That is, instead of providing all possible lagged input and output terms to be terminal variables, a back-shift operator is implemented, q^{-1} , to the function set (or node set). Thus, the terminal set consists solely of the process input and output signals shifted by a single time sample. The authors worked with rational models and the function set is composed of $\{+, -, \div, \times, \text{POW}, \text{SQRT}, \text{SQR}, \text{EXP}, \text{LOG}, \text{back-shift operators}: q^0, q^{-1}, q^{-2}, q^{-3}\}$. Model parameters are optimised using the *recursive least squares* method. A review of the use of rational models in identification and control problems can be found in Zhu et al. (2015).

Some applications of the MGGP include reliability analysis of the liquefaction potential of soil subjected to seismic loading (Muduli and Das, 2015); rainfall-runoff model for short-range streamflow prediction (Mehr and Nourani, 2017); sewer sediment transport modelling (Safari and Mehr, 2018). Faris et al. (2016) proposed a hybrid approach based on MGGP and CS algorithms for developing three rigorous models for roll force, torque and slab temperature in the hot rolling industrial process. MGGP was applied for finding the structure of the symbolic regression models, then CS was used for parameter estimation. Similar approach was proposed by Braik (2021) using MGGP with *capuchin search algorithm* (CapSA) for modelling an industrial winding process. Kusznir and Smoczek (2022) proposed a multi-objective MGGP approach to identify a dynamical model for an

overhead crane. Both the mean square prediction error and the function complexity were minimised.

3.4 Case study: using MGGP

The tools presented in this section were used to identify a simulated PEA with hysteresis. The optimisation framework is based on the MGGP algorithm and was developed in Python¹ (Castro and Barbosa, 2022).

3.4.1 Theoretical model and dataset

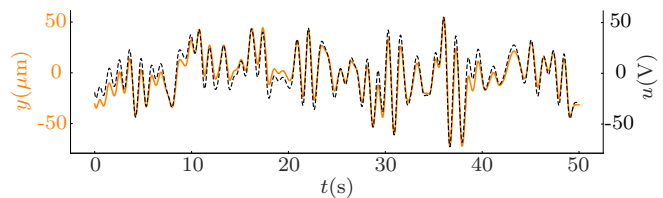
PEAs are used in micro- and nano-positioning applications. This case study considers the PEA with hysteretic nonlinearity modelled by the Bouc-Wen model (Wen, 1976), reviewed in Subsection 2.1, and whose mathematical model is given by (Rakotondrabe, 2011):

$$\begin{cases} \dot{h}(t) = A\dot{u}(t) - \beta|\dot{u}(t)|h(t) - \gamma\dot{u}(t)|h(t)|, \\ y(t) = d_p u(t) - h(t), \end{cases} \quad (30)$$

where $y(t)$ is the displacement, $u(t)$ is the voltage applied to the actuator within the range $-80 \text{ V} \leq u(t) \leq 80 \text{ V}$, $d_p = 1.6 \frac{\mu\text{m}}{\text{V}}$ is the piezoelectric coefficient, $h(t)$ is the hysteretic nonlinear term and $A = 0.9 \frac{\mu\text{m}}{\text{V}}$, $\beta = 0.008 \text{ V}^{-1}$ and $\gamma = 0.008 \text{ V}^{-1}$ are parameters that define the shape and scale of the hysteresis loop.

Model (30) was integrated numerically using a fourth-order Runge-Kutta method with integration step $\delta t = 0.001 \text{ s}$ with the same sampling time $T_s = \delta$ and a sinusoidal input with frequency of 1 Hz is chosen to validate the identified models, i.e., $u(t) = 40 \sin(2\pi t)\text{V}$ (Abreu et al., 2020). The input was a Pseudo random filtered signal (PRFS) with $n_f = 1$, $f_1 = 1 \text{ Hz}$, $v = 1$, $o_1 = 0$, $G_1 = 80$, and $N = N_1 = 50,000$; see Abreu (2021) for a justification of this input. The datasets (see Figure 12) are 50 s long ($N = 50,000$ samples).

Figure 12 Training data for the PEA identification process (see online version for colours)



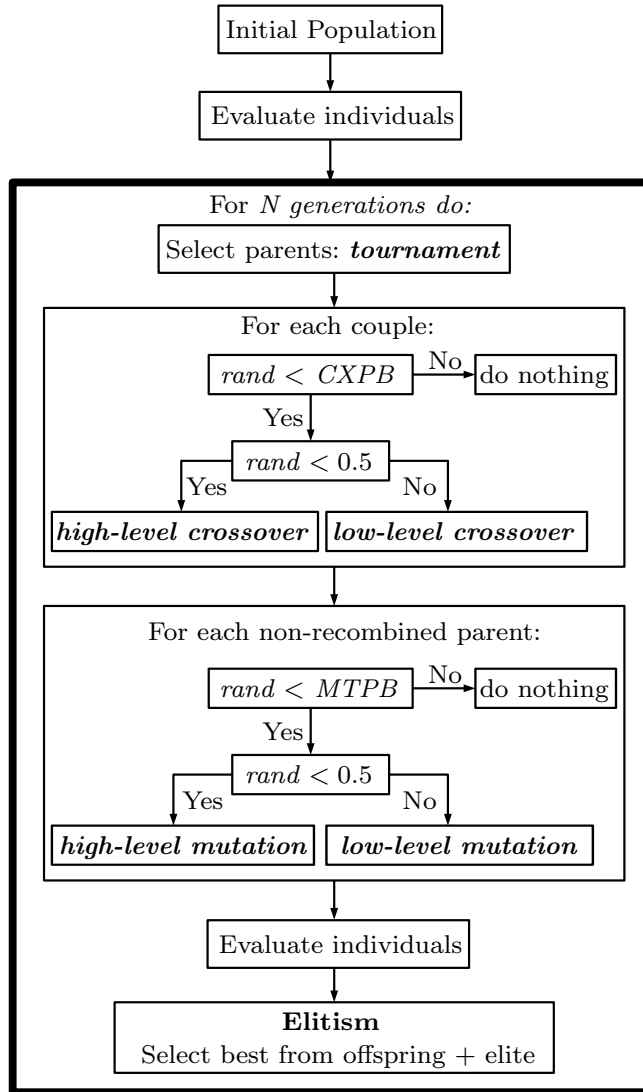
Notes: (- -) input, and (—) output.

3.4.2 Algorithm setup

The MGGP evolutionary framework used to optimise the NARX models was introduced in Castro and Barbosa (2022) and is summarised in Figure 13. In Subsection 3.3.3, we stated that the MGGP works with two-level recombination operators. Similarly, this framework implements a two-level mutation operator with:

- 1 a low-level mutation, which occurs as a GP subtree mutation
- 2 a high-level mutation, which swaps a gene for a new one, with an entirely new basis function.

Figure 13 MGGP algorithm flowchart



Source: Castro and Barbosa (2022)

The following parameters were set:

- *Population size* = 500.
- *Crossover probability (CXPB)* = 0.8 – Defines the probability of a pair of individuals being combined through a recombination operator.
- *Mutation probability (MTPB)* = 0.2 – Defines the probability of a single individual being mutated through a mutation operator if it has not experienced recombination.
- *Maximum GP height* = 5 – Limits the size of a GP tree regarding its height.
- *Maximum number of terms* = 15.

- *Elite size* = 10% – Defines the percentage of individuals that can remain in the next generation.
- *Primitive functions* = $\{\times, \Phi_1, \Phi_2, q^{-1}, q^{-2}, q^{-3}\}$ – The set of functions and *back-shift operators* (responsible for the automatic time lag determination) used as *nodes* in GP individuals. For this experiment, the definitions of the inputs $\phi_{1,k}$ and $\phi_{2,k}$ used by Abreu et al. (2020) were modified. They are going to be functions included in the primitive set that receive as arguments two lagged input variables:

$$\begin{aligned} \Phi_1(u_{k-\tau_1}, u_{k-\tau_2}) &= u_{k-\tau_1} - u_{k-\tau_2}, \\ \Phi_2(u_{k-\tau_1}, u_{k-\tau_2}) &= \text{sign}(\Phi_1(u_{k-\tau_1}, u_{k-\tau_2})). \end{aligned} \quad (31)$$

That will be refer to them as Φ -functions and disregard the subscript k since their structure will not be limited to the difference between the first two lagged inputs (u_{k-1} and u_{k-2}). Figure 14 presents an example of a model term built using all the primitive set $\{\times, \Phi_1, \Phi_2, q^{-1}, q^{-2}, q^{-3}\}$ and the terminal set $\{u_{k-1}, y_{k-1}\}$. This GP individual represents a model term function $g(\varphi) = y_{k-1}\Phi_1(u_{k-2}, u_{k-5})\Phi_2(u_{k-1}, u_{k-3})$ and has a height of 5, with Φ_1 and Φ_2 defined in equation (31).

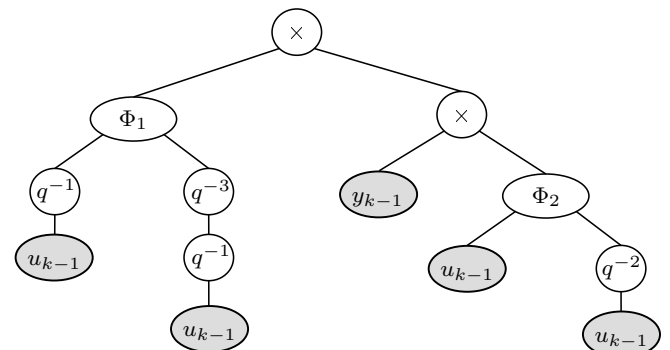
Finally, an *evaluation* (or *cost*) function must be defined to assess model performance. PEM and MS approaches will be compared. Parameter estimation is performed via LS, as defined in equation (27), and the fitness metric is the mean squared error over the different simulations. The evaluation function is generically defined as:

```

Evaluation(individual):
  theta := parameter_estimation(y,u)
  ypred := simulation_method(theta,y,u)
  return fitness(y,ypred)
  
```

where y and u are the training data. The algorithm is run for 200 generations in both simulation cases.

Figure 14 MGGP gene example using the primitive set $\{\times, \Phi_1, \Phi_2, q^{-1}, q^{-2}, q^{-3}\}$ and the terminal set $\{u_{k-1}, y_{k-1}\}$



3.4.3 Results

The estimated models are:

$$\begin{aligned} \mathcal{M}_{PEM} = & \theta_1 u_{k-1} u_{k-4} y_{k-1} + \theta_2 u_{k-2} u_{k-4} \\ & + \theta_3 u_{k-3} y_{k-1} + \theta_4 u_{k-1} y_{k-1} \Phi_2(u_{k-4}, u_{k-6}) \\ & + \theta_5 u_{k-1} y_{k-1} + \theta_6 y_{k-1} + \theta_7 y_{k-3} \\ & + \theta_8 \Phi_2(u_{k-1}, u_{k-8}) + \theta_9 \Phi_2(u_{k-1}, u_{k-3}) \\ & + \theta_{10} \Phi_2(u_{k-1}, u_{k-2}) + \theta_{11} \Phi_2(u_{k-5}, u_{k-1}) \\ & + \theta_{12} \Phi_2(u_{k-5}, u_{k-2}) + \theta_{13} y_{k-2} + \theta_{14} u_{k-1} \\ & + \theta_{15} u_{k-4}, \end{aligned} \quad (32)$$

and

$$\begin{aligned} \mathcal{M}_{MS} = & \theta_1 y_{k-2} u_{k-1} u_{k-3} + \theta_2 u_{k-5} \\ & + \theta_3 u_{k-1} u_{k-5} y_{k-5} + \theta_4 u_{k-1} u_{k-3}^2 \\ & + \theta_5 u_{k-5} y_{k-4} \Phi_2(u_{k-4}, u_{k-1}) \\ & + \theta_6 u_{k-5} y_{k-1} \Phi_2(u_{k-3}, u_{k-1}) \\ & + \theta_7 y_{k-1} + \theta_8 \Phi_1(u_{k-5}, u_{k-1}) \\ & + \theta_9 \Phi_2(u_{k-4}, u_{k-6}) \\ & + \theta_{10} y_{k-3} y_{k-8} \Phi_2(u_{k-4}, u_{k-1}) \\ & + \theta_{11} y_{k-5} y_{k-8} \Phi_2(u_{k-4}, u_{k-1}) \\ & + \theta_{12} u_{k-3}^2 \Phi_2(u_{k-4}, u_{k-1}) + \theta_{13} u_{k-1}^2 u_{k-3} \\ & + \theta_{14} u_{k-1} u_{k-4} \Phi_2(u_{k-5}, u_{k-1}) + \theta_{15} u_{k-10}. \end{aligned} \quad (33)$$

It is worth mentioning that both models have included the Φ -functions which is consistent with the fact that the system has hysteresis. However, it is remarkable that these functions were not imposed during model identification, they were automatically defined (arguments) and selected by the algorithm to improve the simulation performance. Unlike in Abreu (2021) where the additional regressors $\phi_{i,k}$ were used as candidate inputs to the model. Here implementing the Φ -functions allowed the algorithm to build models with a wide variety of differences between two lagged inputs, e.g., $u_{k-1} - u_{k-3}$ and $u_{k-1} - u_{k-8}$, without the need for defining such regressors *a priori*, which avoids dimensionality issues.

Figure 15 shows free-run simulations over the validation data and Table 1 shows the mean absolute percentage error (MAPE). Notice that the experiment using PEM approach yielded model \mathcal{M}_{PEM} (32) that does not represent the hysteresis loop correctly and presents the worst performance. Hence, such a model was not considered in static analysis. Model \mathcal{M}_{MS} (33) with parameters estimated via LS presents a decreasing output when the input becomes constant during *unloading*; see Figure 15(c). Hence, it does not display a *continuum of steady-state solutions*, which is an important feature in the static response of hysteretic systems, as discussed previously.

The continuum of steady-state solutions condition can be verified if the sum of all parameters of all linear output regressors is equal to 1 (i.e., the cluster coefficient $\Sigma_y = 1$) and if $\Sigma_{y^q} = 0$ for $q > 1$, $\Sigma_{u^m} = 0 \forall m$, and $\Sigma_{y^p u^m} = 0 \forall p, m$. Such constraints can be imposed using the CLS estimator equation (28). Considering the input $u_k = \bar{u}$, $\forall k$, it is known that $\Phi_1(\bar{u}, \bar{u}) = \Phi_2(\bar{u}, \bar{u}) = 0$. Hence, the

parameters of model \mathcal{M}_{MS} (33) should comply with the following constraints:

$$\begin{cases} \Sigma_y = \theta_7 = 1, \\ \Sigma_u = \theta_2 + \theta_{15} = 0, \\ \Sigma_{u^3} = \theta_4 + \theta_{13} = 0, \\ \Sigma_{yu^2} = \theta_1 + \theta_3 = 0. \end{cases} \quad (34)$$

Table 2 presents the resulting parameters of model \mathcal{M}_{MS} estimated by CLS, which now attains the *continuum of steady-state property*; see Figure 15(c).

Figure 15 Free-run validation of models \mathcal{M}_{PEM} (....) and \mathcal{M}_{MS} (- - -) with parameters estimated via LS, and model (19) (...), (a) hysteresis loop (b) output displacement (c) output displacement for the cases in which the input becomes constant during *loading* and *unloading*: (—) the system output and (—) the output of \mathcal{M}_{MS} with parameters estimated via CLS (see online version for colours)

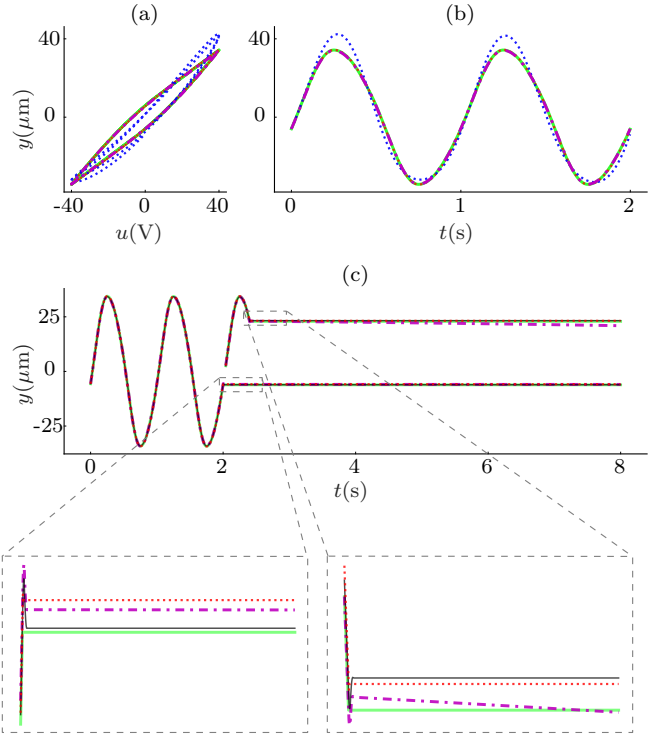


Table 1 Model performance for free-run simulation

Model	MAPE	
	Training	Validation
\mathcal{M}_{PEM} [LS]	2.813	4.077
\mathcal{M}_{MS} [LS]	0.165	0.147
\mathcal{M}_{MS} [CLS]	0.261	0.202
Equation (19) [CLS]	0.440	0.241

We compare models \mathcal{M}_{MS} and equation (19), both estimated with CLS. The former performed better in a free-run simulation over training and validation dynamical data; see Figure 15(b). The static response – when the input becomes constant – during *loading* the steady-state

error was approximately $0.034 \mu\text{m}$ against $0.276 \mu\text{m}$; see Figure 15(c). As for the static response during *unloading*, both models yielded similar performances, with steady-state error of about $0.353 \mu\text{m}$ and $0.287 \mu\text{m}$ for models \mathcal{M}_{MS} and equation (19), respectively.

Table 2 Model parameters obtained with LS or CLS

Model	Values	
\mathcal{M}_{PEM} [LS]	$\theta_1 = 1.4909 \times 10^{-11}$	$\theta_2 = 5.4779 \times 10^{-10}$
	$\theta_3 = -7.6907 \times 10^{-9}$	$\theta_4 = 7.9000 \times 10^{-10}$
	$\theta_5 = 6.9281 \times 10^{-9}$	$\theta_6 = 2.9993$
	$\theta_7 = 9.9950 \times 10^{-1}$	$\theta_8 = -1.2043 \times 10^{-6}$
	$\theta_9 = 6.7605 \times 10^{-5}$	$\theta_{10} = -7.8538 \times 10^{-5}$
	$\theta_{11} = -1.1553 \times 10^{-5}$	$\theta_{12} = -1.6279 \times 10^{-7}$
	$\theta_{13} = -2.9988$	$\theta_{14} = 4.0921 \times 10^{-5}$
	$\theta_{15} = -4.0806 \times 10^{-5}$	
	$\theta_1 = -5.5315 \times 10^{-5}$	$\theta_2 = -9.2096 \times 10^{-2}$
	$\theta_3 = 5.5510 \times 10^{-5}$	$\theta_4 = -1.5447 \times 10^{-4}$
	$\theta_5 = 5.9861 \times 10^{-3}$	$\theta_6 = -5.9610 \times 10^{-3}$
	$\theta_7 = 0.9999$	$\theta_8 = -3.0283 \times 10^{-1}$
	$\theta_9 = -6.7148 \times 10^{-4}$	$\theta_{10} = 5.5376 \times 10^{-3}$
	$\theta_{11} = -5.5476 \times 10^{-3}$	$\theta_{12} = -1.5676 \times 10^{-5}$
	$\theta_{13} = 1.5431 \times 10^{-4}$	$\theta_{14} = -1.8981 \times 10^{-9}$
	$\theta_{15} = 9.2068 \times 10^{-2}$	
\mathcal{M}_{MS} [CLS]	$\theta_1 = -4.0204 \times 10^{-5}$	$\theta_2 = -9.9779 \times 10^{-2}$
	$\theta_3 = 4.0205 \times 10^{-5}$	$\theta_4 = -1.1382 \times 10^{-4}$
	$\theta_5 = 5.7168 \times 10^{-3}$	$\theta_6 = -5.6884 \times 10^{-3}$
	$\theta_7 = 1.0000$	$\theta_8 = -3.1411 \times 10^{-1}$
	$\theta_9 = -9.0632 \times 10^{-4}$	$\theta_{10} = 5.1940 \times 10^{-3}$
	$\theta_{11} = -5.2046 \times 10^{-3}$	$\theta_{12} = -1.7847 \times 10^{-5}$
	$\theta_{13} = 1.1382 \times 10^{-4}$	$\theta_{14} = -7.6848 \times 10^{-7}$
	$\theta_{15} = 9.9779 \times 10^{-2}$	

The MGGP is a promising tool for identifying NARX polynomial models. It can find appropriate model regressors in a search space that would be computationally unfeasible for other approaches. Besides, it can be applied in grey-box identification procedures, as demonstrated in this example.

4 Control of hysteretic systems

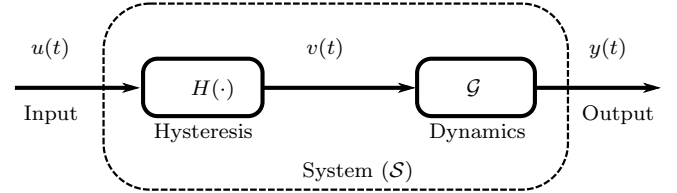
A common goal is to attenuate the hysteretic behaviour of the system (Visone, 2008; Chaoui and Gualous, 2016; Yi et al., 2019) prior to feedback control design. It is often assumed that hysteretic systems can be represented as shown in Figure 16 (Peng and Chen, 2013; Gu et al., 2016b), where \mathcal{G} describes the linear behaviour of the system \mathcal{S} , preceded by a model $H(\cdot)$ that describes the hysteretic behaviour (Liu et al., 2010; Gu et al., 2016a). Hence this representation is sometimes called a pseudo-Hammerstein model (Cao and Chen, 2012; Deng et al., 2014) and can be used to describe hysteretic systems modelled either from phenomenological models, such as the Bouc-Wen and the Prandtl-Ishlinskii models, or from grey-box NARX models; see Section 2.

The approaches commonly adopted to design controllers and compensators for hysteretic systems can be classified into three categories:

- 1 compensation approaches
- 2 feedback control
- 3 combination of compensation and feedback control approaches, a key difference being the way they represent hysteretic behaviour (Gu et al., 2016b).

Some of the main trends are reviewed in what follows.

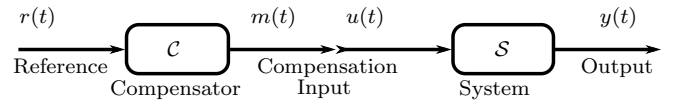
Figure 16 Block diagram of the cascaded model structure used to represent hysteretic systems



4.1 Specific compensation approaches

Compensation-based approaches aim to design an input that mitigates undesirable behaviours, as illustrated in Figure 17.

Figure 17 Block diagram of the compensation approach \mathcal{C} for a hysteretic system \mathcal{S}



One of the approaches to design the compensator \mathcal{C} is through the construction of an inverse function $H^{-1}(\cdot)$ of the hysteresis model $H(\cdot)$, which will provide a compensation input m to mitigate the hysteresis. A common problem to this class of approaches is that often the hysteresis model is not invertible (Rakotondrabe, 2013), as for the case of the Bouc-Wen model. Faced with this problem, Rakotondrabe (2011) proposed an alternative approach that considers the restructuring of the Bouc-Wen model in an *inverse multiplicative scheme* (Wang et al., 2011; Zhou et al., 2012; Hassani et al., 2014). Compensation schemes without the need for complete inversion based on the inverse multiplicative scheme have also been proposed (Rakotondrabe, 2012; Li et al., 2014; Al Janaideh et al., 2017).

Operator-based models of hysteresis have been widely used for compensation because their inverse can be determined (Peng and Chen, 2013). Although the Preisach model is not analytically invertible, its inverse can be approximated numerically (Song et al., 2005; Ruderman and Bertram, 2010).

On the other hand, the Prandtl-Ishlinskii hysteresis model has the advantage of being analytically invertible (Krejci and Kuhnen, 2001; Kuhnen and Janocha, 2001; Mokaberi and Requicha, 2008; Rakotondrabe et al., 2010; Al Janaideh et al., 2011, 2016).

4.2 Identification-based compensation

Not every hysteretic system can be represented by structures such as the Bouc-Wen and the Prandtl-Ishlinskii models (Rakotondrabe, 2011; Gu et al., 2012). Also, there are some challenges related to the estimation of their parameters (Peng and Chen, 2013; Hassani et al., 2014). A promising alternative (see Subsection 2.2) is provided by grey-box identification of NARX models, which can be tailored to reproduce specific features and thus making them effective for use in a compensation scheme. Unfortunately the literature on the use of NARX models in the compensation of hysteresis is still scarce (Leva and Piroddi, 2002; Dong and Tan, 2014; Lacerda Júnior et al., 2019; Abreu et al., 2020; Abreu, 2021; Tavares et al., 2022).

There are basically two mainstreams: in *model-based control* the aim is to identify a model from data and subsequently to design a compensator \mathcal{C} using the identified model, akin to Subsection 4.1. A second way, called *data-driven control*, is to directly identify the compensator \mathcal{C} from data.

In the realm of *model-based control*, few works have been dedicated to the search for NARX models that are suitable for compensation. Accurate models (Leva and Piroddi, 2002; Lacerda Júnior et al., 2019) are not always appropriate for compensation [Abreu, (2021), Subsection 3.2.1]. Solutions to this situation have been proposed. Using the identified model it is possible to find a control signal that will yield the desired dynamics by

- 1 iteratively computing the roots of a model-based polynomial (Abreu, 2021; Tavares et al., 2022)
- 2 careful structure selection to enable that the compensation input can be isolated when the identified model is rewritten as a compensator (Abreu et al., 2020; Abreu, 2021).

Following this design philosophy, Zhu and co-workers applied the U-model to control systems with rational models (Zhu et al., 2018).

Some works on *data-driven control* have addressed the design of compensators using operator-based hysteresis models, such as the Preisach and the Prandtl-Ishlinskii models (Croft et al., 1999; Gu et al., 2012; Qin et al., 2013). Basically, the core idea revolves around modifications that are carried out in the model, such as structure specifications, changes in the input mapping function of the inverse model, among others. When it comes to the use of NARX models for this type of compensation, very few papers have been found on this topic. Li and Chen (2013) proposed the design of a nonlinear adaptive NARX neural compensator that is adjusted online. Dong and Tan (2014) adopted an operator proposed by Deng and Tan (2009) to capture the change tendency of the hysteresis behaviour, but now with the aim of mapping the inverse hysteresis behaviour. Thus, the output of this inverse hysteretic operator is used as an additional candidate regressor $\phi_{i,k}$ for identifying a NARX polynomial model (12) that estimates the input \hat{u}_k rather than the output signal y_k of the hysteretic system. A

common challenge in identifying the compensator directly from data is to avoid potential causality problems. Ways of dealing with this, and a methodology for hysteretic systems, have been discussed in Abreu et al. (2020) and Abreu (2021).

Example 4.1: Details concerning this example can be found in Abreu et al. (2020), Abreu (2021) and Tavares et al. (2021, 2022). The experimental dataset has been presented² in Abreu et al. (2020). The following three NARX compensators were designed to mitigate hysteresis nonlinearity in an experimental pneumatic control valve. The first one \mathcal{C}_R is given in the form of polynomials in the control action m_k . Hence the roots of such polynomials are the control action that achieves the goal. In cases with more than one root, the choice is made as discussed in Abreu (2021, Definition 4.2). The polynomials that compose \mathcal{C}_R are:

$$\begin{aligned} & 3.76m_k^2 + [0.119 - 3.76m_{k-1} - 4.73r_{k-1}]m_k + 0.976r_k \\ & + 0.024r_{k-1} - r_{k+1} + [4.73r_{k-1} - 0.119]m_{k-1} = 0, \\ & \text{for } m_k > m_{k-1}, \end{aligned} \quad (35)$$

and

$$\begin{aligned} & -3.76m_k^2 + [0.119 + 3.76m_{k-1} + 4.73r_{k-1}]m_k \\ & + 0.976r_k + 0.024r_{k-1} - r_{k+1} \\ & - [4.73r_{k-1} + 0.119]m_{k-1} = 0, \text{ for } m_k < m_{k-1}. \end{aligned} \quad (36)$$

The last two compensators referred to as \mathcal{C}_I and $\check{\mathcal{C}}$ are, respectively, given by:

$$\begin{aligned} m_k = & \frac{1}{19.32}[r_{k+1} - r_k \\ & + 19.32m_{k-1} + 19.76[m_{k-1} - m_{k-2}] \\ & - 9.44 \operatorname{sign}(m_{k-1} - m_{k-2})[m_{k-1} - m_{k-2}]m_{k-1} \\ & + 12.61 \operatorname{sign}(m_{k-1} - m_{k-2})[m_{k-1} - m_{k-2}]r_k], \end{aligned} \quad (37)$$

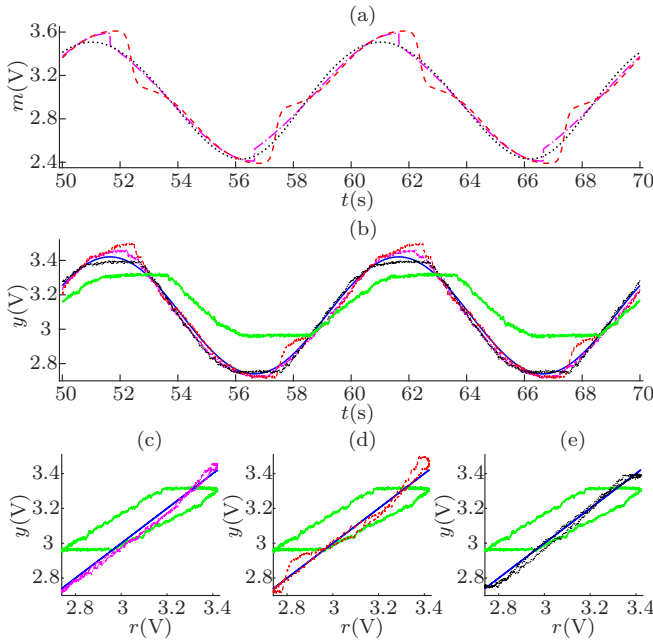
and

$$\begin{aligned} \check{m}_k = & \check{m}_{k-1} + 86.67[r_{k+1} - r_k] - 85.02[r_k - r_{k-1}] \\ & - 0.98[r_{k+1} - r_k]r_k \\ & + 1.72 \operatorname{sign}(r_k - r_{k-1})[r_k - r_{k-1}]r_k \\ & - 1.13 \operatorname{sign}(r_k - r_{k-1})[r_k - r_{k-1}]\check{m}_{k-1}. \end{aligned} \quad (38)$$

The control actions in this case are obtained simply by computing the difference equations that compose \mathcal{C}_I and $\check{\mathcal{C}}$. The results of applying the designed compensators to the experimental pneumatic valve for a sinusoidal input signal, are shown in Figure 18.

From Figure 18 it is clearly seen that the three compensators significantly reduce the tracking error when compared to the uncompensated system.

Figure 18 Experimental compensation for the pneumatic valve with sampling time of $T_s = 0.01$ s, (—) compensator \mathcal{C}_R (35)–(36), (---) compensator \mathcal{C}_I (37), (...) compensator $\check{\mathcal{C}}$ (38), (a) compensation inputs for \mathcal{C}_R , \mathcal{C}_I and $\check{\mathcal{C}}$ (b) valve responses, hysteresis loops uncompensated and compensated with (c) \mathcal{C}_R (d) \mathcal{C}_I (e) $\check{\mathcal{C}}$ (see online version for colours)

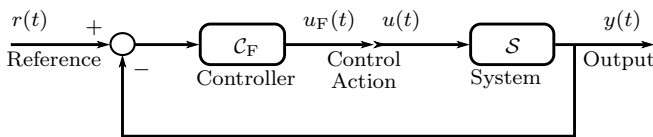


Notes: In Figures 18(b)–18(d): (—) the system output without compensation, and (—) the reference $r = 0.34 \sin(0.2\pi t) + 3.08$ V.

4.3 Feedback control approaches

Because compensation approaches work in open loop, they are prone to a number of problems related to parameter and structure uncertainty (Peng and Chen, 2013). Feedback control approaches (Figure 19) aim at handling such uncertainties.

Figure 19 Block diagram of the feedback control approach \mathcal{C}_F for a hysteretic system \mathcal{S}



Many feedback control approaches have been developed based on linear and nonlinear control techniques to deal with hysteretic systems (Zhou et al., 2004; Ikhouane and Rodellar, 2006; Payam et al., 2009; Riccardi et al., 2013, 2014; Cheng et al., 2015). The choice of which control technique to use depends on the purpose and how the control problem is formulated. When it is desired to handle both transient and steady-state responses, the proportional-integral-derivative (PID) control technique is

one of the most used and accepted options in both academic and industrial fields (Ang et al., 2005; Ikhouane and Rodellar, 2006; Riccardi et al., 2012, 2013, 2014).

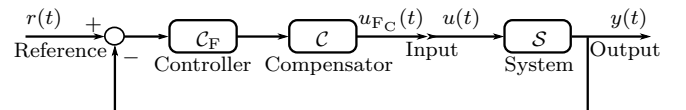
In the realm of robust feedback controllers, especially \mathcal{H}_2 and \mathcal{H}_∞ methods (Doyle et al., 1989), have been considered in the context of hysteresis (Salapaka et al., 2002; Chuang and Petersen, 2013; Ahmad et al., 2017). This approach commonly considers the hysteresis as a bounded disturbance in the nominal model of the system and adjusts the control law by optimising an objective function that minimises the \mathcal{H}_2 or \mathcal{H}_∞ norm.

In the context of nonlinear techniques, *backstepping* was used in Payam et al. (2009). With this technique, the control law and the Lyapunov function to ensure stability are constructed systematically (Khalil, 2002). *Sliding mode control*, which is robust to uncertainties and disturbances (Edwards and Spurgeon, 1998), was used to attenuate hysteresis (Liaw et al., 2007; Xu and Li, 2009). Other control techniques, such as those based on neural networks (Liaw and Shirinzadeh, 2009) and adaptive control (Tao and Kokotovic, 1995; Chen et al., 2008), have also been applied to the feedback control of these systems. A large number of modifications and combinations of these techniques to control hysteretic systems have been investigated (Zhou et al., 2004; Feng et al., 2005; Ikhouane et al., 2005; Zhou and Wen, 2008; Zhang et al., 2017b; Chen and Hisayama, 2008; Zheng et al., 2014; Mansourfar and Baradarannia, 2018).

4.4 Feedback control with compensation

Although feedback control approaches offer advantages that are superior to compensation, the presence of uncertainties together with hard nonlinearities might degrade the performance of such controllers (Peng and Chen, 2013). Therefore, it is often advantageous to combine both. Hence, one of the compensation approaches presented in Subsections 4.1 and 4.2 can be used to construct an *inverse hysteresis model*, i.e., compensator, that is cascaded with the system to make the relationship between its input and output signals more linear. Thereafter, a feedback controller (Subsection 4.3) is designed, as illustrated in Figure 20. Many works have dealt with this problem (Ge and Jouaneh, 1996; Song et al., 2005; Shen et al., 2008; Peng and Chen, 2010; Cao et al., 2013; Schindeler and Aschemann, 2013; Liu et al., 2014).

Figure 20 Block diagram of the compensator \mathcal{C} combined with feedback controller \mathcal{C}_F



In the field of linear control, studies regarding the use of compensator with linear techniques, such as PID and \mathcal{H}_2 , have reported a considerable increase in control performance (Ge and Jouaneh, 1996; Peng and Chen, 2010; Song et al., 2005). Sliding mode and backstepping control,

were combined with the use of compensators to handle hysteretic systems in Shen et al. (2008) and Schinelle and Aschemann (2013). Open challenges include stability analysis of these control schemes (Gu et al., 2016b).

5 Conclusions

This work briefly surveyed problems and advances related to the identification and control of hysteretic systems. The work began by presenting the literature review on modelling of hysteretic systems. Some of the classic phenomenological models of hysteresis, already established in the literature, were briefly contextualised, with emphasis on the Bouc-Wen model and the Prandtl-Ishlinskii operator. Aiming at a more comprehensive model, not limited to describing only the hysteresis nonlinearity, some of the main concepts and definitions based on the NARX philosophy were addressed, whose model class can be built using black-box or grey-box identification techniques. A more general NARX polynomial representation that fits the grey-box scenario is formalised when it is assumed that the auxiliary information can be converted as a new class of regressors that can optionally be included in the model. Ways of determining from data a class of regressors especially well-suited for hysteretic systems were discussed. Works that use NARX models for hysteretic systems were reviewed, with a critical eye on the proposed ways to enable such models to represent some subtle aspects of hysteresis. Also, some properties of hysteretic systems, as well as alternative ways and guidelines for achieving them using grey-box NARX models, which correspond to interesting topics to be pursued in the future, were discussed.

Also tools for building NARX polynomial models in a more general setting were described. Special attention was given to structure selection and parameter estimation problems. Different simulation methods and their implications for structure selection and model validation were also addressed. Metaheuristic algorithms were given special attention because structure selection for NARX polynomial models can be seen as a combinatorial optimisation problem. The computational framework was built using EAs and some related works were mentioned. In terms of hysteresis identification, we introduced an EA called MGGP which has shown promise for identifying NARX polynomial models, as illustrated for a simulated PEA.

In the context of hysteresis control, this work briefly mentioned some commonly used approaches to designing controllers and compensators. Control and hysteresis compensation based on the Bouc-Wen, the Prandtl-Ishlinskii and the NARX models were addressed and divided into three categories:

- 1 compensators
- 2 feedback controllers
- 3 the combination of both.

The effectiveness of three recently proposed approaches to design compensators for general dynamical systems, and also for hysteretic systems, represented by NARX polynomial models, was illustrated using experimental tests. In addition, some control challenges that remain open were presented, as well as some advantages and limitations found in existing control approaches in the literature to deal with hysteresis.

Acknowledgements

The authors acknowledge financial support from the Conselho Nacional de Desenvolvimento Científico e Tecnológico (Grant 142194/2017-4, PEOGBA; 03412/2019-4, LAA; 309404/2021-5, BHGB), from FAPEMIG (Grant PPM-00337-17 and TEC-1217/98) and from Coordenação de Aperfeiçoamento de Pessoal de Nível Superior (Code 001, HCC).

References

- Abdullah, N.H.S., Karsiti, M.N. and Ibrahim, R. (2012) ‘A review of pH neutralization process control’, in *4th International Conference on Intelligent and Advanced Systems (ICIAS)*, Vol. 2, pp.594–598, Kuala Lumpur, Malaysia [online] <https://doi.org/10.1109/ICIAS.2012.6306084>.
- Abreu, P.E.O.G.B. (2021) *Identification and Compensator Design using NARX Models*, PhD thesis, Escola de Engenharia, Universidade Federal de Minas Gerais, Belo Horizonte [online] <http://hdl.handle.net/1843/40199>.
- Abreu, P.E.O.G.B., Dreke, V.D.R., Aguirre, L.A. and Garcia, C. (2021) ‘Enabling invariant models to describe time-varying dynamics: a case study’, *IFAC-PapersOnLine*, *3rd IFAC Conference on Modelling, Identification and Control of Nonlinear Systems*, Tokyo, Japan, Vol. 54, No. 14, pp.1–6 [online] <https://doi.org/10.1016/j.ifacol.2021.10.319>.
- Abreu, P.E.O.G.B., Tavares, L.A., Teixeira, B.O.S. and Aguirre, L.A. (2020) ‘Identification and nonlinearity compensation of hysteresis using NARX models’, *Nonlinear Dynamics*, Vol. 102, No. 1, pp.285–301 [online] <https://doi.org/10.1007/s11071-020-05936-5>.
- Aguirre, L.A., Corrêa, M.V. and Cassini, C.C.S. (2002) ‘Nonlinearities in NARX polynomial models: representation and estimation’, *IEE Proceedings – Control Theory and Applications*, Vol. 149, No. 4, pp.343–348 [online] <https://doi.org/10.1049/ip-cta:20020398>.
- Aguirre, L.A. (2014) ‘Identification of smooth nonlinear dynamical systems with non-smooth steady-state features’, *Automatica*, Vol. 50, No. 4, pp.1160–1166 [online] <https://doi.org/10.1016/j.automatica.2014.02.012>.
- Aguirre, L.A. (2019) *A Bird’s Eye View of Nonlinear System Identification*, arXiv:1907.06803v4 [eess.SY] [online] <https://doi.org/10.48550/arXiv.1907.06803>.
- Aguirre, L.A., Barbosa, B.H.G. and Braga, A.P. (2010) ‘Prediction and simulation errors in parameter estimation for nonlinear systems’, *Mechanical Systems and Signal Processing*, Vol. 24, No. 8, pp.2855–2867 [online] <https://doi.org/10.1016/j.ymssp.2010.05.003>.

- Aguirre, L.A. and Billings, S.A. (1994) 'Validating identified nonlinear models with chaotic dynamics', *International Journal of Bifurcation and Chaos*, Vol. 4, No. 1, pp.109–125 [online] <https://doi.org/10.1142/S0218127494000095>.
- Aguirre, L.A. and Billings, S.A. (1995) 'Improved structure selection for nonlinear models based on term clustering', *International Journal of Control*, Vol. 62, No. 3, pp.569–587 [online] <https://doi.org/10.1080/00207179508921557>.
- Aguirre, L.A. and Mendes, E.M.A.M. (1996) 'Global nonlinear polynomial models: structure, term clusters and fixed points', *International Journal of Bifurcation and Chaos*, Vol. 6, No. 2, pp.279–294 [online] <https://doi.org/10.1142/S0218127496000059>.
- Ahmad, I. (2018) 'Two degree-of-freedom robust digital controller design with Bouc-Wen hysteresis compensator for piezoelectric positioning stage', *IEEE Access*, Vol. 6, pp.17275–17283 [online] <https://doi.org/10.1109/ACCESS.2018.2815924>.
- Ahmad, I., Abdurraqeb, A.M. and Ahmad, W. (2017) 'Modern H-infinity control design for ultra-precise micro/nanopositioning with hysteresis compensation', in *9th IEEE-GCC Conference and Exhibition (GCCCE)*, Manama, Bahrain, pp.1–6 [online] <https://doi.org/10.1109/IEEEGCC.2017.8448087>.
- Al-Bender, F., Symens, W., Swevers, J. and Van Brussel, H. (2004) 'Theoretical analysis of the dynamic behavior of hysteresis elements in mechanical systems', *International Journal of Non-linear Mechanics*, Vol. 39, No. 10, pp.1721–1735 [online] <https://doi.org/10.1016/j.ijnonlinmec.2004.04.005>.
- Al Janaideh, M., Rakheja, S. and Su, C-Y. (2011) 'An analytical generalized Prandtl-Ishlinskii model inversion for hysteresis compensation in micropositioning control', *IEEE/ASME Transactions on Mechatronics*, Vol. 16, No. 4, pp.734–744 [online] <https://doi.org/10.1109/TMECH.2010.2052366>.
- Al Janaideh, M., Rakotondrabe, M. and Aljanaideh, O. (2016) 'Further results on hysteresis compensation of smart micropositioning systems with the inverse Prandtl-Ishlinskii compensator', *IEEE Transactions on Control Systems Technology*, Vol. 24, No. 2, pp.428–439 [online] <https://doi.org/10.1109/TCST.2015.2446959>.
- Al Janaideh, M., Su, C-Y. and Rakheja, S. (2008) 'Development of the rate-dependent Prandtl-Ishlinskii model for smart actuators', *Smart Materials and Structures*, Vol. 17, No. 3, p.35026 [online] <https://dx.doi.org/10.1088/0964-1726/17/3/035026>.
- Ali, I.B., Naouar, M.W. and Monmasson, E. (2021) 'Parameters identification for a photovoltaic module: comparison between PSO, GA and CS metaheuristic optimisation algorithms', *International Journal of Modelling, Identification and Control*, Vol. 38, Nos. 3–4, pp.211–230 [online] <https://doi.org/10.1504/IJMIC.2021.123378>.
- Aljanaideh, O., Rakotondrabe, M., Al-Darabsah, I., Aljanaideh, K.F. and Al Janaideh, M. (2017) 'A model-based feedforward hysteresis compensator for micropositioning control', in *American Control Conference (ACC)*, Seattle, WA, USA, pp.3506–3511 [online] <https://doi.org/10.23919/ACC.2017.7963489>.
- Ang, K.H., Chong, G. and Li, Y. (2005) 'PID control system analysis, design, and technology', *IEEE Transactions on Control Systems Technology*, Vol. 13, No. 4, pp.559–576 [online] <https://doi.org/10.1109/TCST.2005.847331>.
- Ayala, H.V.H., Habineza, D., Rakotondrabe, M., Klein, C.E. and Coelho, L.S. (2015) 'Nonlinear black-box system identification through neural networks of a hysteretic piezoelectric robotic micromanipulator', *IFAC-PapersOnLine*, Vol. 48, No. 28, pp.409–414 [online] <https://doi.org/10.1016/j.ifacol.2015.12.162>.
- Baeza, J.R. and Garcia, C. (2018) 'Friction compensation in pneumatic control valves through feedback linearization', *Journal of Control, Automation and Electrical Systems*, Vol. 29, No. 3, pp.303–317 [online] <https://doi.org/10.1007/s40313-018-0382-y>.
- Baldacchino, T., Anderson, S.R. and Kadirkamanathan, V. (2013) 'Computational system identification for Bayesian NARMAX modelling', *Automatica*, Vol. 49, No. 9, pp.2641–2651 [online] <https://doi.org/10.1016/j.automatica.2013.05.023>.
- Banks, H.T., Kurdila, A.J. and Webb, G. (1997) 'Identification of hysteretic control influence operators representing smart actuators part I: formulation', *Mathematical Problems in Engineering*, Vol. 3, No. 4, pp.287–328 [online] <https://doi.org/10.1155/S1024123X97000586>.
- Barbosa, A.M., Takahashi, R.H.C. and Aguirre, L.A. (2015) 'Equivalence of nonlinear model structures based on Pareto uncertainty', *IET Control Theory & Applications*, Vol. 9, No. 16, pp.2423–2429 [online] <https://doi.org/10.1049/iet-cta.2015.0408>.
- Barbosa, B.H.G., Aguirre, L.A. and Braga, A.P. (2019) 'Piecewise affine identification of a hydraulic pumping system using evolutionary computation', *IET Control Theory & Applications*, Vol. 13, No. 9, pp.1394–1403 [online] <https://doi.org/10.1049/iet-cta.2018.5621>.
- Barbosa, B.H.G., Aguirre, L.A., Martinez, C.B. and Braga, A.P. (2011) 'Black and gray-box identification of a hydraulic pumping system', *IEEE Transactions on Control Systems Technology*, Vol. 19, No. 2, pp.398–406 [online] <https://doi.org/10.1109/TCST.2010.2042600>.
- Barroso, M.F., Takahashi, R.H.C. and Aguirre, L.A. (2007) 'Multi-objective parameter estimation via minimal correlation criterion', *J. Proc. Control*, Vol. 17, No. 4, pp.321–332 [online] <https://doi.org/10.1016/j.jprocont.2006.10.005>.
- Bashash, S. and Jalili, N. (2006) 'Underlying memory-dominant nature of hysteresis in piezoelectric materials', *Journal of Applied Physics*, Vol. 100, No. 1, p.14103 [online] <https://doi.org/10.1063/1.2208805>.
- Bequette, B.W. (1991) 'Nonlinear control of chemical processes: a review', *Industrial & Engineering Chemistry Research*, Vol. 30, No. 7, pp.1391–1413 [online] <https://doi.org/10.1021/ie00055a001>.
- Berenyi, P., Horvath, G., Lampaert, V. and Swevers, J. (2005) 'Nonlocal hysteresis function identification and compensation with neural networks', *IEEE Transactions on Instrumentation and Measurement*, Vol. 54, No. 6, pp.2227–2238 [online] <https://doi.org/10.1109/TIM.2005.858822>.
- Bernstein, D.S. (2007) 'Ivory ghost [ask the experts]', *IEEE Control Systems Magazine*, Vol. 27, No. 5, pp.16–17 [online] <https://doi.org/10.1109/MCS.2007.903688>.
- Beza, M. and Bongiorno, M. (2014) 'Application of recursive least squares algorithm with variable forgetting factor for frequency component estimation in a generic input signal', *IEEE Transactions on Industry Applications*, Vol. 50, No. 2, pp.1168–1176 [online] <https://doi.org/10.1109/TIA.2013.2279195>.
- Bhadra, S., Panda, A. and Bhowmick, P. (2019a) 'A nonlinear model-based control scheme for benchmark industrial processes', in *International Conference on Opto-Electronics and Applied Optics (Optronix)*, pp.1–5, Kolkata, India [online] <https://doi.org/10.1109/OPTRONIX.2019.8862325>.

- Bhadra, S., Panda, A. and Bhowmick, P. (2019b) 'Model-based adaptive control scheme for benchmark pH-neutralisation process', in *International Conference on Ubiquitous and Emerging Concepts on Sensors and Transducers (UEMCOS)*, Kolkata, India, pp.1–6 [online] <https://doi.org/10.1109/UEMCOS46508.2019.9221586>.
- Biagiola, S.I., Agamennoni, O.E. and Figueroa, J.L. (2016) 'Robust control of Wiener systems: application to a pH neutralization process', *Brazilian Journal of Chemical Engineering*, Vol. 33, No. 1, pp.145–153 [online] <https://doi.org/10.1590/0104-6632.20160331s00002846>.
- Bianchi, F., Breschi, V., Piga, D. and Piroddi, L. (2021) 'Model structure selection for switched NARX system identification: a randomized approach', *Automatica*, Vol. 125, No. 109415 [online] <https://doi.org/10.1016/j.automatica.2020.109415>.
- Bianchi, F., Falsone, A., Prandini, M. and Piroddi, L. (2016) 'A randomized approach for NARX model identification based on a multivariate Bernoulli distribution', *Int. J. of Systems Science*, Vol. 48, No. 6, pp.1203–1216 [online] <https://doi.org/10.1080/00207721.2016.1244309>.
- Billings, S.A. (2013) *Nonlinear System Identification: NARMAX Methods in the Time, Frequency, and Spatio-Temporal Domains*, John Wiley & Sons.
- Billings, S.A. and Aguirre, L.A. (1995) 'Effects of the sampling time on the dynamics and identification of nonlinear models', *International Journal of Bifurcation and Chaos*, Vol. 5, No. 6, pp.1541–1556 [online] <https://doi.org/10.1142/S0218127495001174>.
- Billings, S.A. and Chen, S. (1989a) 'Extended model set, global data and threshold model identification of severely non-linear systems', *International Journal of Control*, Vol. 50, No. 5, pp.1897–1923 [online] <https://doi.org/10.1080/00207178908953473>.
- Billings, S.A. and Chen, S. (1989b) 'Identification of non-linear rational systems using a prediction-error estimation algorithm', *International Journal of Systems Science*, Vol. 20, No. 3, pp.467–494 [online] <https://doi.org/10.1080/00207728908910143>.
- Billings, S.A., Chen, S. and Korenberg, M.J. (1989) 'Identification of MIMO non-linear systems using a forward-regression orthogonal estimator', *International Journal of Control*, Vol. 49, No. 6, pp.2157–2189 [online] <https://doi.org/10.1080/00207178908559767>.
- Billings, S.A. and Zheng, G.L. (1999) 'Qualitative validation of radial basis function networks', *Mechanical Systems and Signal Processing*, Vol. 13, No. 2, pp.335–349 [online] <https://doi.org/10.1006/mssp.1998.0189>.
- Bouc, R. (1971) 'Modèle Mathématique d'hystérésis (a mathematical model for hysteresis)', *Acustica*, Vol. 21, No. 1, pp.16–25.
- Braik, M. (2021) 'A hybrid multi-gene genetic programming with capuchin search algorithm for modeling a nonlinear challenge problem: modeling industrial winding process, case study', *Neural Processing Letters*, Vol. 53, No. 4, pp.2873–2916 [online] <https://doi.org/10.1007/s11063-021-10530-w>.
- Brewick, P.T., Masri, S.F., Carboni, B. and Lacarbonara, W. (2016) 'Data-based nonlinear identification and constitutive modeling of hysteresis in NiTiNOL and steel strands', *Journal of Engineering Mechanics*, Vol. 142, No. 12, p.4016107 [online] [https://doi.org/10.1061/\(ASCE\)EM.1943-7889.0001170](https://doi.org/10.1061/(ASCE)EM.1943-7889.0001170).
- Brokate, M. and Sprekels, J. (1996) *Hysteresis and Phase Transitions*, Springer-Verlag, New York [online] <https://doi.org/10.1007/978-1-4612-4048-8>.
- Cao, K., Li, R., Du, H. and Ma, J. (2019) 'Modeling and compensation of symmetric hysteresis in piezoceramic actuators', *Results in Physics*, Vol. 13, p.102095 [online] <https://doi.org/10.1016/j.rinp.2019.02.031>.
- Cao, Y. and Chen, X.B. (2012) 'A novel discrete ARMA-based model for piezoelectric actuator hysteresis', *IEEE/ASME Transactions on Mechatronics*, Vol. 17, No. 4, pp.737–744 [online] <https://doi.org/10.1109/TMECH.2011.2128339>.
- Cao, Y., Cheng, L., Chen, X.B. and Peng, J.Y. (2013) 'An inversion-based model predictive control with an integral-of-error state variable for piezoelectric actuators', *IEEE/ASME Transactions on Mechatronics*, Vol. 18, No. 3, pp.895–904 [online] <https://doi.org/10.1109/TMECH.2012.2194792>.
- Carboni, B., Lacarbonara, W., Brewick, P.T. and Masri, S.F. (2018) 'Dynamical response identification of a class of nonlinear hysteretic systems', *Journal of Intelligent Material Systems and Structures*, Vol. 29, No. 13, pp.1–16 [online] <https://doi.org/10.1177/1045389X18778792>.
- Castro, H.C. and Barbosa, B.H.G. (2022) *A Python Library for Nonlinear System Identification using Multi-gene Genetic Programming Algorithm*, arXiv:2211.05723v1 [online] <https://doi.org/10.48550/arXiv.2211.05723>.
- Chan, R.W.K., Yuen, J.K.K., Lee, E.W.M. and Arashpour, M. (2015) 'Application of nonlinear-autoregressive-exogenous model to predict the hysteretic behaviour of passive control systems', *Engineering Structures*, Vol. 85, pp.1–10 [online] <https://doi.org/10.1016/j.engstruct.2014.12.007>.
- Chaoui, H. and Gualous, H. (2016) 'Adaptive control of piezoelectric actuators with hysteresis and disturbance compensation', *Journal of Control, Automation and Electrical Systems*, Vol. 27, No. 6, pp.579–586 [online] <https://doi.org/10.1007/s40313-016-0270-2>.
- Charalampakis, A.E. (2010) 'Parameters of bouc-wen hysteretic model revisited', in *Proceedings of the 9th HSTAM International Congress on Mechanics*, Limassol, Cyprus, pp.1–8.
- Chen, Q., Worden, K., Peng, P. and Leung, A. (2007) 'Genetic algorithm with an improved fitness function for (N)ARX modelling', *Mechanical Systems and Signal Processing*, Vol. 21, No. 2, pp.994–1007 [online] <https://doi.org/10.1016/j.ymssp.2006.01.011>.
- Chen, S. and Billings, S.A. (1989) 'Representations of non-linear systems: the NARMAX model', *International Journal of Control*, Vol. 49, No. 3, pp.1013–1032 [online] <https://doi.org/10.1080/00207178908559683>.
- Chen, S., Billings, S.A. and Luo, W. (1989) 'Orthogonal least squares methods and their application to non-linear system identification', *International Journal of Control*, Vol. 50, No. 5, pp.1873–1896 [online] <https://doi.org/10.1080/00207178908953472>.
- Chen, X. and Hisayama, T. (2008) 'Adaptive sliding-mode position control for piezo-actuated stage', *IEEE Transactions on Industrial Electronics*, Vol. 55, No. 11, pp.3927–3934 [online] <https://doi.org/10.1109/TIE.2008.926768>.
- Chen, X., Su, C-Y. and Fukuda, T. (2008) 'Adaptive control for the systems preceded by hysteresis', *IEEE Transactions on Automatic Control*, Vol. 53, No. 4, pp.1019–1025 [online] <https://doi.org/10.1109/TAC.2008.919551>.
- Cheng, L., Liu, W., Hou, Z-G., Yu, J. and Tan, M. (2015) 'Neural-network-based nonlinear model predictive control for piezoelectric actuators', *IEEE Transactions on Industrial Electronics*, Vol. 62, No. 12, pp.7717–7727 [online] <https://doi.org/10.1109/TIE.2015.2455026>.

- Choudhury, M.A.A.S., Shah, S.L. and Thornhill, N.F. (2008) *Diagnosis of Process Nonlinearities and Valve Stiction: Data Driven Approaches*, Springer, Berlin, Heidelberg [online] <https://doi.org/10.1007/978-3-540-79224-6>.
- Chuang, N. and Petersen, I.R. (2013) 'Robust H^∞ control of hysteresis in a piezoelectric stack actuator', *Journal of Dynamic Systems, Measurement, and Control*, Vol. 135, No. 6, p.64501 [online] <https://doi.org/10.1115/1.4024811>.
- Croft, D., Shed, G. and Devasia, S. (1999) 'Creep, hysteresis, and vibration compensation for piezoactuators: atomic force microscopy application', *Journal of Dynamic Systems, Measurement, and Control*, Vol. 123, No. 1, pp.35–43 [online] <https://doi.org/10.1115/1.1341197>.
- de Almeida, L.A.L., Deep, G.S., Lima, A.M.N. and Neff, H. (2003) 'Limiting loop proximity hysteresis model', *IEEE Transactions on Magnetics*, Vol. 39, No. 1, pp.523–528 [online] <https://doi.org/10.1109/TMAG.2002.806344>.
- de Morais, G.A., Barbosa, B.H.G., Ferreira, D.D. and Paiva, L.S. (2019) 'Soft sensors design in a petrochemical process using an evolutionary algorithm', *Measurement*, Vol. 148, p.106920 [online] <https://doi.org/10.1016/j.measurement.2019.106920>.
- Deng, L. and Tan, Y. (2009) 'Modeling hysteresis in piezoelectric actuators using NARMAX models', *Sensors and Actuators A: Physical*, Vol. 149, No. 1, pp.106–112 [online] <https://doi.org/10.1016/j.sna.2008.09.022>.
- Deng, L., Yang, P., Xue, Y. and Lv, X. (2014) 'NARMAX model based pseudo-Hammerstein identification for rate-dependent hysteresis', in *Fifth International Conference on Intelligent Control and Information Processing*, Dalian, China, pp.155–162 [online] <https://doi.org/10.1109/ICICIP.2014.7010331>.
- Domínguez-González, A., Stiharu, I. and Sedaghati, R. (2014) 'Practical hysteresis model for magnetorheological dampers', *Journal of Intelligent Material Systems and Structures*, Vol. 25, No. 8, pp.967–979 [online] <https://doi.org/10.1177/1045389X13502867>.
- Dong, R. and Tan, Y. (2014) 'Inverse hysteresis modeling and nonlinear compensation of ionic polymer metal composite sensors', in *11th World Congress on Intelligent Control and Automation*, Shenyang, China, pp.2121–2125 [online] <https://doi.org/10.1109/WCICA.2014.7053049>.
- Doyle, J., Glover, K., Khargonekar, P. and Francis, B. (1989) 'State-space solutions to standard \mathcal{H}_2 and \mathcal{H}_∞ control problems', *IEEE Transactions on Automatic Control*, Vol. 34, No. 8, pp.831–847 [online] <https://doi.org/10.1109/9.29425>.
- Draper, N.R. and Smith, H. (1998) *Applied Regression Analysis*, 3rd ed., John Wiley & Sons, New York.
- Drincic, B. and Bernstein, D.S. (2009) 'A multiplay model for rate-independent and rate-dependent hysteresis with nonlocal memory', in *48th IEEE Conference on Decision and Control (CDC)*, Shenyang, China, pp.8381–8386 [online] <https://doi.org/10.1109/CDC.2009.5400874>.
- Edwards, C. and Spurgeon, S. (1998) *Sliding Mode Control: Theory and Applications*, 1st ed., CRC Press, London [online] <https://doi.org/10.1201/9781498701822>.
- Eiben, A.E. and Smith, J.E. (2015) *Introduction to Evolutionary Computing*, 2nd ed., Springer-Verlag, Berlin, Heidelberg, Bristol, UK [online] <https://doi.org/10.1007/978-3-662-44874-8>.
- Esbrook, A., Tan, X. and Khalil, H.K. (2013) 'Control of systems with hysteresis via servocompensation and its application to nanopositioning', *IEEE Transactions on Control Systems Technology*, Vol. 21, No. 3, pp.725–738 [online] <https://doi.org/10.1109/TCST.2012.2192734>.
- Esbrook, A., Tan, X. and Khalil, H.K. (2014) 'Inversion-free stabilization and regulation of systems with hysteresis via integral action', *Automatica*, Vol. 50, No. 4, pp.1017–1025 [online] <https://doi.org/10.1016/j.automatica.2013.11.013>.
- Eskinat, E., Johnson, S.H. and Luyben, W.L. (1993) 'Use of auxiliary information in system identification', *Industrial & Engineering Chemistry Research*, Vol. 32, No. 9, pp.1981–1992 [online] <https://doi.org/10.1021/ie00021a021>.
- Fagundes, L.P., Morais, A.S., Oliveira-Lopes, L.C. and Morais, J.S. (2022) 'Enhanced algorithm for randomised model structure selection', *Int. J. of Systems Science*, Vol. 53, No. 5, pp.1090–1109 [online] <https://doi.org/10.1080/00207721.2021.1988755>.
- Falsone, A., Piroddi, L. and Prandini, M. (2015) 'A randomized algorithm for nonlinear model structure selection', *Automatica*, Vol. 60, pp.227–238 [online] <https://doi.org/10.1016/j.automatica.2015.07.023>.
- Faris, H., Sheta, A.F. and Öznergiz, E. (2016) 'MGP-CC: a hybrid multigene GP-Cuckoo search method for hot rolling manufacture process modelling', *Systems Science & Control Engineering*, Vol. 4, No. 1, pp.39–49 [online] <https://doi.org/10.1080/21642583.2015.1124032>.
- Feng, Y., Wu, Y.-X., Hu, Y.-M. and Su (2005) 'Adaptive backstepping control of a class of uncertain nonlinear systems with Prandtl-Ishlinskii hysteresis', in *International Conference on Machine Learning and Cybernetics*, Guangzhou, China, Vol. 2, pp.697–701 [online] <https://doi.org/10.1109/ICMLC.2005.1527034>.
- Freitas, L., Barbosa, B.H.G. and Aguirre, L.A. (2021) 'Including steady-state information in nonlinear models: an application to the development of soft-sensors', *Engineering Applications of Artificial Intelligence*, Vol. 102, p.104253 [online] <https://doi.org/10.1016/j.engappai.2021.104253>.
- Fu, J., Liao, G., Yu, M., Li, P. and Lai, J. (2016) 'NARX neural network modeling and robustness analysis of magnetorheological elastomer isolator', *Smart Materials and Structures*, Vol. 25, No. 12, p.125019 [online] <https://dx.doi.org/10.1088/0964-1726/25/12/125019>.
- Fujii, F., Tatebatake, K., Morita, K. and Shiinoki, T. (2018) 'A Bouc-Wen model-based compensation of the frequency-dependent hysteresis of a piezoelectric actuator exhibiting odd harmonic oscillation', *Actuators*, Vol. 7, No. 3, p.37 [online] <https://doi.org/10.3390/act7030037>.
- Ge, P. and Jouaneh, M. (1995) 'Modeling hysteresis in piezoceramic actuators', *Precision Engineering*, Vol. 17, No. 3, pp.211–221 [online] [https://doi.org/10.1016/0141-6359\(95\)00002-U](https://doi.org/10.1016/0141-6359(95)00002-U).
- Ge, P. and Jouaneh, M. (1996) 'Tracking control of a piezoceramic actuator', *IEEE Transactions on Control Systems Technology*, Vol. 4, No. 3, pp.209–216 [online] <https://doi.org/10.1109/87.491195>.
- Gebraad, P.M.O., van Wingerden, J., Fleming, P.A. and Wright, A.D. (2013) 'LPV identification of wind turbine rotor vibrational dynamics using periodic disturbance basis functions', *IEEE Transactions on Control Systems Technology*, Vol. 21, No. 4, pp.1183–1190 [online] <https://doi.org/10.1109/TCST.2013.2257775>.
- Ghosh, S. and Maka, S. (2011) 'Genetic algorithm based narx model identification for evaluation of insulin sensitivity', *Applied Soft Computing*, Vol. 11, No. 1, pp.221–226 [online] <https://doi.org/10.1016/j.asoc.2009.11.012>.

- Goldberg, D.E. and Holland, J.H. (1988) 'Genetic algorithms and machine learning', *Machine Learning*, Vol. 3, No. 2, pp.95–99 [online] <https://doi.org/10.1023/A:1022602019183>.
- Gu, G.Y., Yang, M.J. and Zhu, L.M. (2012) 'Real-time inverse hysteresis compensation of piezoelectric actuators with a modified Prandtl-Ishlinskii model', *Review of Scientific Instruments*, Vol. 83, No. 6, p.65106 [online] <https://doi.org/10.1063/1.4728575>.
- Gu, G-Y., Zhu, L-M. and Su, C-Y. (2014) 'Modeling and compensation of asymmetric hysteresis nonlinearity for piezoceramic actuators with a modified Prandtl-Ishlinskii model', *IEEE Transactions on Industrial Electronics*, Vol. 61, No. 3, pp.1583–1595 [online] <https://doi.org/10.1109/TIE.2013.2257153>.
- Gu, G-Y., Li, C-X., Zhu, L-M. and Su, C-Y. (2016a) 'Modeling and identification of piezoelectric-actuated stages cascading hysteresis nonlinearity with linear dynamics', *IEEE/ASME Transactions on Mechatronics*, Vol. 21, No. 3, pp.1792–1797 [online] <https://doi.org/10.1109/TMECH.2015.2465868>.
- Gu, G-Y., Zhu, L-M., Su, C-Y., Ding, H. and Fatikow, S. (2016b) 'Modeling and control of piezo-actuated nanopositioning stages: a survey', *IEEE Transactions on Automation Science and Engineering*, Vol. 13, No. 1, pp.313–332 [online] <https://doi.org/10.1109/TASE.2014.2352364>.
- Gu, Y. and Wei, H.L. (2018) 'A robust model structure selection method for small sample size and multiple datasets problems', *Information Sciences*, Vols. 451–452, pp.195–209 [online] <https://doi.org/10.1016/j.ins.2018.04.007>.
- Ha, J-L., Fung, R-F. and Yang, C-S. (2005) 'Hysteresis identification and dynamic responses of the impact drive mechanism', *Journal of Sound and Vibration*, Vol. 283, Nos. 3–5, pp.943–956 [online] <https://doi.org/10.1016/j.jsv.2004.05.032>.
- Hafiz, F., Swain, A. and Mendes, E.M.A.M. (2020a) 'Multi-objective evolutionary framework for non-linear system identification: a comprehensive investigation', *Neurocomputing*, Vol. 386, pp.257–280 [online] <https://doi.org/10.1016/j.neucom.2019.12.095>.
- Hafiz, F., Swain, A., Mendes, E.M.A.M. and Aguirre, L.A. (2020b) 'Multiobjective evolutionary approach to grey-box identification of buck converter', *IEEE Transactions on Circuits and Systems I: Regular Papers*, Vol. 67, No. 6, pp.2016–2028 [online] <https://doi.org/10.1109/TCSI.2020.2970759>.
- Hassani, V., Tjahjowidodo, T. and Do, T.N. (2014) 'A survey on hysteresis modeling, identification and control', *Mechanical Systems and Signal Processing*, Vol. 49, Nos. 1–2, pp.209–233 [online] <https://doi.org/10.1016/j.ymssp.2014.04.012>.
- Haynes, B.R. and Billings, S.A. (1992) 'Method for the global analysis of non-linear parametrized systems', *International Journal of Control*, Vol. 55, No. 2, pp.457–482 [online] <https://doi.org/10.1080/00207179208934249>.
- Herrera, F., Lozano, M. and Verdegay, J.L. (1998) 'Tackling real-coded genetic algorithms: operators and tools for behavioural analysis', *Artificial Intelligence Review*, Vol. 12, No. 4, pp.265–319 [online] <https://doi.org/10.1023/A:1006504901164>.
- Hinchliffe, M.P. and Willis, M.J. (2003) 'Dynamic systems modelling using genetic programming', *Computers & Chemical Engineering*, Vol. 27, No. 12, pp.1841–1854 [online] <https://doi.org/10.1016/j.compchemeng.2003.06.001>.
- Hong, T., Morris, A.J., Karim, M.N., Zhang, J. and Luo, W. (1996) 'Nonlinear control of a wastewater pH neutralisation process using adaptive NARX models', in *International Conference on Systems, Man and Cybernetics. Information Intelligence and Systems*, Beijing, China, Vol. 2, pp.911–916 [online] <https://doi.org/10.1109/ICSMC.1996.571178>.
- Hong, X., Mitchell, R.J., Chen, S., Harris, C.J., Li, K. and Irwin, G.W. (2008) 'Model selection approaches for non-linear system identification: a review', *International Journal of Systems Science*, Vol. 39, No. 10, pp.925–946 [online] <https://doi.org/10.1080/00207720802083018>.
- Hu, H. and Ben Mrad, R. (2003) 'On the classical Preisach model for hysteresis in piezoceramic actuators', *Mechatronics*, Vol. 13, No. 2, pp.85–94 [online] [https://doi.org/10.1016/S0957-4158\(01\)00043-5](https://doi.org/10.1016/S0957-4158(01)00043-5).
- Ikhouane, F., Mañosa, V. and Rodellar, J. (2005) 'Adaptive control of a hysteretic structural system', *Automatica*, Vol. 41, No. 2, pp.225–231 [online] <https://doi.org/10.1016/j.automatica.2004.08.018>.
- Ikhouane, F. and Rodellar, J. (2006) 'A linear controller for hysteretic systems', *IEEE Transactions on Automatic Control*, Vol. 51, No. 2, pp.340–344 [online] <https://doi.org/10.1109/TAC.2005.863511>.
- Ikhouane, F. and Rodellar, J. (2007) *Systems with Hysteresis: Analysis, Identification and Control Using the Bouc-Wen Model*, John Wiley & Sons.
- Isermann, R. and Münchhof, M. (2011) *Identification of Dynamic Systems: An Introduction with Applications*, 1st ed., Springer-Verlag, Berlin, Heidelberg, New York [online] <https://doi.org/10.1007/978-3-540-78879-9>.
- Ismail, M., Ikhouane, F. and Rodellar, J. (2009) 'The hysteresis Bouc-Wen model, a survey', *Archives of Computational Methods in Engineering*, Vol. 16, No. 2, pp.161–188 [online] <https://doi.org/10.1007/s11831-009-9031-8>.
- Jankowski, K., Marszał, M. and Stefański, A. (2017) 'Formulation of presliding domain non-local memory hysteretic loops based upon modified maxwell slip model', *Tribology Letters*, Vol. 65, No. 2, p.56 [online] <https://doi.org/10.1007/s11249-017-0838-4>.
- Ji, W., Lv, D., Lv, Q., Yuan, J., Rong, L. and Zhu, L. (2021) 'Research on vibration compensation control of electromagnetic bearings rotor', *International Journal of Modelling, Identification and Control*, Vol. 39, No. 4, pp.279–284 [online] <https://doi.org/10.1504/IJMIC.2021.123786>.
- Joshi, A.K. (1987) 'An introduction to tree adjoining grammars', in Manaster-Ramer, A. (Eds.): *Mathematics of Language*, Vol. 1, pp.87–115, John Benjamins [online] <https://doi.org/10.1075/z.35.07jos>.
- Joshi, A.K. and Schabes, Y. (1997) 'Tree-adjoining grammars', in Rozenberg, G. and Salomaa, A. (Eds.): *Handbook of Formal Languages*, pp.69–123, Springer, Berlin, Heidelberg [online] <https://doi.org/10.1007/978-3-642-59126-6-2>.
- Kallmeyer, L. (2009) 'A declarative characterization of different types of multicomponent tree adjoining grammars', *Research on Language and Computation*, Vol. 7, No. 1, pp.55–99 [online] <https://doi.org/10.1007/s11168-009-9064-z>.
- Karami, K., Westwick, D. and Schoukens, J. (2021) 'Applying polynomial decoupling methods to the polynomial NARX model', *Mechanical Systems and Signal Processing*, Vol. 148, p.107134 [online] <https://doi.org/10.1016/j.ymssp.2020.107134>.
- Keesman, K.J. (2011) *System Identification: An Introduction*, 1st ed., Springer-Verlag London, New York [online] <https://doi.org/10.1007/978-0-85729-522-4>.

- Khalid, M., Yusof, R., Joshani, M., Selamat, H. and Joshani, M. (2014) ‘Nonlinear identification of a magneto-rheological damper based on dynamic neural networks’, *Computer-Aided Civil and Infrastructure Engineering*, Vol. 29, No. 3, pp.221–233 [online] <https://doi.org/10.1111/mice.12005>.
- Khalil, H.K. (2002) *Nonlinear Systems*, 3rd ed., Prentice-Hall, Upper Saddle River, New Jersey.
- Khandelwal, D., Schoukens, M. and Tóth, R. (2019a) ‘Data-driven modelling of dynamical systems using tree adjoining grammar and genetic programming’, in *IEEE Congress on Evolutionary Computation (CEC)*, pp.2673–2680, Wellington, New Zealand [online] <https://doi.org/10.1109/CEC.2019.8790250>.
- Khandelwal, D., Schoukens, M. and Tóth, R. (2019b) ‘Grammar-based representation and identification of dynamical systems’, in *18th European Control Conference (ECC)*, pp.1318–1323, Naples, Italy [online] <https://doi.org/10.23919/ECC.2019.8795719>.
- Koo, T-K.J. (1995) ‘Model reference adaptive fuzzy control of robot manipulator’, in *IEEE International Conference on Systems, Man and Cybernetics. Intelligent Systems for the 21st Century*, Vancouver, Canada, Vol. 1, pp.424–429 [online] <https://doi.org/10.1109/ICSMC.1995.537796>.
- Koza, J.R. (1994) ‘Genetic programming as a means for programming computers by natural selection’, *Statistics and Computing*, Vol. 4, No. 2, pp.87–112 [online] <https://doi.org/10.1007/BF00175355>.
- Krejci, P. and Kuhnen, K. (2001) ‘Inverse control of systems with hysteresis and creep’, *IEE Proceedings – Control Theory and Applications*, Vol. 148, No. 3, pp.185–192 [online] <https://doi.org/10.1049/ip-cta:20010375>.
- Kuhnen, K. (2003) ‘Modeling, identification and compensation of complex hysteretic nonlinearities: a modified Prandtl-Ishlinskii approach’, *European Journal of Control*, Vol. 9, No. 4, pp.407–418 [online] <https://doi.org/10.3166/ejc.9.407-418>.
- Kuhnen, K. and Janocha, H. (2001) ‘Inverse feedforward controller for complex hysteretic nonlinearities in smart-material systems’, *Control and Intelligent Systems*, Vol. 29, No. 3, pp.74–83.
- Kusznir, T. and Smoczek, J. (2022) ‘Multi-gene genetic programming-based identification of a dynamic prediction model of an overhead traveling crane’, *Sensors*, Vol. 22, No. 1, p.339 [online] <https://doi.org/10.3390/s22010339>.
- Kyprianou, A., Worden, K. and Panet, M. (2001) ‘Identification of hysteretic systems using the differential evolution algorithm’, *Journal of Sound and Vibration*, Vol. 248, No. 2, pp.289–314 [online] <https://doi.org/10.1006/jsvi.2001.3798>.
- Lacerda Júnior, W.R., Martins, S.A.M. and Nepomuceno, E.G. (2017) ‘Influence of sampling rate and discretization methods in the parameter identification of systems with hysteresis’, *Journal of Applied Nonlinear Dynamics*, Vol. 6, No. 4, pp.509–520 [online] <http://dx.doi.org/10.5890/JAND.2017.12.006>.
- Lacerda Júnior, W.R., Martins, S.A.M., Nepomuceno, E.G. and Lacerda, M.J. (2019) ‘Control of hysteretic systems through an analytical inverse compensation based on a NARX model’, *IEEE Access*, Vol. 7, pp.98228–98237 [online] <https://doi.org/10.1109/ACCESS.2019.2926057>.
- Larico, E.R.E. and Garcia, C. (2019) ‘Predictive controller applied to a pH neutralization process’, *IFAC-PapersOnLine*, Vol. 52, No. 1, pp.202–206 [online] <https://doi.org/10.1016/j.ifacol.2019.06.062>.
- Le Guisquet, S. and Amabili, M. (2021a) ‘Identification by means of a genetic algorithm of nonlinear damping and stiffness of continuous structures subjected to large-amplitude vibrations. Part I: single-degree-of-freedom responses’, *Mechanical Systems and Signal Processing*, Vol. 153, p.107470 [online] <https://doi.org/10.1016/j.ymssp.2020.107470>.
- Le Guisquet, S. and Amabili, M. (2021b) ‘Identification by means of a genetic algorithm of nonlinear damping and stiffness of continuous structures subjected to large-amplitude vibrations. Part II: one-to-one internal resonances’, *Mechanical Systems and Signal Processing*, Vol. 161, p.107972 [online] <https://doi.org/10.1016/j.ymssp.2021.107972>.
- Leontaritis, I.J. and Billings, S.A. (1985a) ‘Input-output parametric models for non-linear systems part I: deterministic non-linear systems’, *International Journal of Control*, Vol. 41, No. 2, pp.303–328 [online] <https://doi.org/10.1080/0020718508961129>.
- Leontaritis, I.J. and Billings, S.A. (1985b) ‘Input-output parametric models for non-linear systems part II: stochastic non-linear systems’, *International Journal of Control*, Vol. 41, No. 2, pp.329–344 [online] <https://doi.org/10.1080/0020718508961130>.
- Letellier, C., Ménard, O. and Aguirre, L.A. (2002) ‘Validation of selected global models’, in Soofi, A.S. and Cao, L. (Eds.): *Modelling and Forecasting Financial Data, Studies in Computational Finance*, Vol. 2, pp.283–302, Springer, Boston, MA [online] https://doi.org/10.1007/978-1-4615-0931-8_14.
- Leva, A. and Piroddi, L. (2002) ‘NARX-based technique for the modelling of magneto-rheological damping devices’, *Smart Materials and Structures*, Vol. 11, No. 1, pp.79–88 [online] <https://dx.doi.org/10.1088/0964-1726/11/1/309>.
- Li, C.J. and Jeon, Y. (1993) ‘Genetic algorithm in identifying non-linear auto regressive with exogenous input models for non-linear systems’, In *American Control Conference*, San Francisco, CA, USA, pp.2305–2309 [online] <https://doi.org/10.23919/ACC.1993.4793298>.
- Li, W. and Chen, X. (2013) ‘Compensation of hysteresis in piezoelectric actuators without dynamics modeling’, *Sensors and Actuators A: Physical*, Vol. 199, pp.89–97 [online] <https://doi.org/10.1016/j.sna.2013.04.036>.
- Li, Z., Su, C-Y. and Chai, T. (2014) ‘Compensation of hysteresis nonlinearity in magnetostrictive actuators with inverse multiplicative structure for Preisach model’, *IEEE Transactions on Automation Science and Engineering*, Vol. 11, No. 2, pp.613–619 [online] <https://doi.org/10.1109/TASE.2013.2284437>.
- Liaw, H.C. and Shirinzadeh, B. (2009) ‘Neural network motion tracking control of piezo-actuated flexure-based mechanisms for micro-/nanomanipulation’, *IEEE/ASME Transactions on Mechatronics*, Vol. 14, No. 5, pp.517–527 [online] <https://doi.org/10.1109/TMECH.2009.2005491>.
- Liaw, H.C., Shirinzadeh, B. and Smith, J. (2007) ‘Enhanced sliding mode motion tracking control of piezoelectric actuators’, *Sensors and Actuators A: Physical*, Vol. 138, No. 1, pp.194–202 [online] <https://doi.org/10.1016/j.sna.2007.04.062>.
- Liu, L. and Yang, Y. (2015) *Modeling and Precision Control of Systems with Hysteresis*, 1st ed., Butterworth-Heinemann [online] <https://doi.org/10.1016/C2014-0-04804-6>.
- Liu, S., Su, C. and Li, Z. (2014) ‘Robust adaptive inverse control of a class of nonlinear systems with Prandtl-Ishlinskii hysteresis model’, *IEEE Transactions on Automatic Control*, Vol. 59, No. 8, pp.2170–2175 [online] <https://doi.org/10.1109/TAC.2014.2298732>.

- Liu, Y-T., Chang, K-M. and Li, W-Z. (2010) ‘Model reference adaptive control for a piezo-positioning system’, *Precision Engineering*, Vol. 34, No. 1, pp.62–69 [online] <https://doi.org/10.1016/j.precisioneng.2009.03.006>.
- Ljung, L. (1999) *System Identification: Theory for the User*, 2nd ed., Prentice Hall, New Jersey.
- Madár, J., Abonyi, J. and Szeifert, F. (2005) ‘Genetic programming for the identification of nonlinear input-output models’, *Industrial & Engineering Chemistry Research*, Vol. 44, No. 9, pp.3178–3186 [online] <https://doi.org/10.1021/ie049626e>.
- Mansourfar, S. and Baradarannia, M. (2018) ‘Adaptive sliding mode control of a system with Bouc-Wen model’, in *11th International Symposium on Mechatronics and its Applications (ISMA)*, Sharjah, UAE, No. 1, pp.1–5 [online] <https://doi.org/10.1109/ISMA.2018.8330122>.
- Martins, S.A.M. (2016) *Modelos Auto Regressivos para Representação de Sistemas com Histerese*, PhD thesis, Escola de Engenharia, Universidade Federal de Minas Gerais, Belo Horizonte [online] <http://hdl.handle.net/1843/BUBD-AAQF6D>.
- Martins, S.A.M. and Aguirre, L.A. (2016) ‘Sufficient conditions for rate-independent hysteresis in autoregressive identified models’, *Mechanical Systems and Signal Processing*, Vol. 75, pp.607–617 [online] <https://doi.org/10.1016/j.ymssp.2015.12.031>.
- Masri, S.F., Caffrey, J.P., Caughey, T.K., Smyth, A.W. and Chassiakos, A.G. (2004) ‘Identification of the state equation in complex non-linear systems’, *International Journal of Non-Linear Mechanics*, Vol. 39, No. 7, pp.1111–1127 [online] [https://doi.org/10.1016/S0020-7462\(03\)00109-4](https://doi.org/10.1016/S0020-7462(03)00109-4).
- Mayergoyz, I.D. (2003) *Mathematical Models of Hysteresis and Their Applications* Elsevier Science, New York [online] <https://doi.org/10.1016/B978-0-12-480873-7.X5000-2>.
- Mehr, A.D. and Nourani, V. (2017) ‘A Pareto-optimal moving average-multigene genetic programming model for rainfall-runoff modelling’, *Environmental Modelling & Software*, Vol. 92, pp.239–251 [online] <https://doi.org/10.1016/j.envsoft.2017.03.004>.
- Merola, A., Colacino, D., Cosentino, C. and Amato, F. (2015) ‘A parsimonious friction model for efficient identification and compensation of hysteresis with non-local memory’, *International Journal of Modelling, Identification and Control*, Vol. 23, No. 1, pp.85–91 [online] <https://doi.org/10.1504/IJMIC.2015.067497>.
- Mohammadzaheri, M., Grainger, S. and Bazghaleh, M. (2012) ‘A comparative study on the use of black box modelling for piezoelectric actuators’, *The International Journal of Advanced Manufacturing Technology*, Vol. 63, Nos. 9–12, pp.1247–1255 [online] <https://doi.org/10.1007/s00170-012-3987-5>.
- Mokaberi, B. and Requicha, A. (2008) ‘Compensation of scanner creep and hysteresis for AFM nanomanipulation’, *IEEE Transactions on Automation Science and Engineering*, Vol. 5, No. 2, pp.197–206 [online] <https://doi.org/10.1109/TASE.2007.895008>.
- Morris, K.A. (2011) ‘What is hysteresis?’, *Applied Mechanics Reviews*, Vol. 64, No. 5, p.50801 [online] <https://doi.org/10.1115/1.4007112>.
- Muduli, P.K. and Das, S.K. (2015) ‘Model uncertainty of spt-based method for evaluation of seismic soil liquefaction potential using multi-gene genetic programming’, *Soils and Foundations*, Vol. 55, No. 2, pp.258–275 [online] <https://doi.org/10.1016/j.sandf.2015.02.003>.
- Nelles, O. (2001) *Nonlinear System Identification: From Classical Approaches to Neural Networks and Fuzzy Models*, Springer-Verlag, Berlin, Heidelberg [online] <https://doi.org/10.1007/978-3-662-04323-3>.
- Nepomuceno, E.G., Takahashi, R.H.C. and Aguirre, L.A. (2007) ‘Multiobjective parameter estimation for nonlinear systems: affine information and least-squares formulation’, *Int. J. Control.*, Vol. 80, No. 6, p.1–9 [online] <https://doi.org/10.1080/00207170601185053>.
- Ni, Y.Q., Ko, J.M. and Wong, C.W. (1998) ‘Identification of non-linear hysteretic isolators from periodic vibration tests’, *Journal of Sound and Vibration*, Vol. 217, No. 4, pp.737–756 [online] <https://doi.org/10.1006/jsvi.1998.1804>.
- Nnaji, A.C., Holderbaum, W. and Becerra, V. (2021) ‘A novel friction model for predicting nonlinear friction dynamics’, *International Journal of Modelling, Identification and Control*, Vol. 38, No. 2, pp.105–120 [online] <https://doi.org/10.1504/IJMIC.2021.122497>.
- Oh, J. and Bernstein, D.S. (2005) ‘Semilinear Duhem model for rate-independent and rate-dependent hysteresis’, *IEEE Transactions on Automatic Control*, Vol. 50, No. 5, pp.631–645 [online] <https://doi.org/10.1109/TAC.2005.847035>.
- Paleologu, C., Benesty, J. and Ciochina, S. (2008) ‘A robust variable forgetting factor recursive least-squares algorithm for system identification’, *IEEE Signal Processing Letters*, Vol. 15, pp.597–600 [online] <https://doi.org/10.1109/LSP.2008.2001559>.
- Parlitz, U., Hornstein, A., Engster, D., Al-Bender, F., Lampkaert, V., Tjahowidodo, T., Fassois, S.D., Rizos, D., Wong, C.X., Worden, K. and Manson, G. (2004) ‘Identification of pre-sliding friction dynamics’, *Chaos*, Vol. 14, No. 2, pp.420–430 [online] <https://doi.org/10.1063/1.1737818>.
- Payam, A.F., Fathioupor, M. and Yazdanpanah, M.J. (2009) ‘A backstepping controller for piezoelectric actuators with hysteresis in nanopositioning’, in *4th IEEE International Conference on Nano/Micro Engineered and Molecular Systems*, Shenzhen, China, pp.711–716 [online] <https://doi.org/10.1109/NEMS.2009.5068678>.
- Pearson, R.K. (1999) *Discrete-Time Dynamic Models*, Oxford University Press, Oxford [online] <https://doi.org/10.1093/oso/9780195121988.001.0001>.
- Peng, J. and Chen, X. (2010) ‘H₂-optimal digital control of piezoelectric actuators’, in *8th World Congress on Intelligent Control and Automation*, Jinan, China, pp.3684–3690 [online] <https://doi.org/10.1109/WCICA.2010.5553921>.
- Peng, J. and Chen, X. (2013) ‘A survey of modeling and control of piezoelectric actuators’, *Modern Mechanical Engineering*, Vol. 3, No. 1, pp.1–20 [online] <http://dx.doi.org/10.4236/mme.2013.31001>.
- Piroddi, L. (2008) ‘Simulation error minimisation methods for NARX model identification’, *International Journal of Modelling, Identification and Control*, Vol. 3, No. 4, pp.392–403 [online] <https://doi.org/10.1504/IJMIC.2008.020548>.
- Piroddi, L. and Spinelli, W. (2003) ‘An identification algorithm for polynomial NARX models based on simulation error minimization’, *International Journal of Control*, Vol. 76, No. 17, pp.1767–1781 [online] <https://doi.org/10.1080/00207170310001635419>.
- Poli, R., Langdon, W.B. and McPhee, N.F. (2008) *A Field Guide to Genetic Programming*, with contributions by J.R. Koza [online] <http://lulu.com>, <http://www.gp-field-guide.org.uk>.

- Pop, E., Ilcea, G. and Buzdugan, S. (2018) 'Use properties of distributions to model the systems with severe nonlinearities', in *CBU International Conference Proceedings*, Prague, Czech Republic, Vol. 6, pp.1150–1157 [online] <https://doi.org/10.12955/cbup.v6.1308>.
- Popiołek, J. (1990) 'Some properties of functions modul and signum', *Formalized Mathematics*, Vol. 1, No. 2, pp.263–264.
- Qin, Y., Tian, Y., Zhang, D., Shirinzadeh, B. and Fatikow, S. (2013) 'A novel direct inverse modeling approach for hysteresis compensation of piezoelectric actuator in feedforward applications', *IEEE/ASME Transactions on Mechatronics*, Vol. 18, No. 3, pp.981–989 [online] <https://doi.org/10.1109/TMECH.2012.2194301>.
- Quaranta, G., Lacarbonara, W. and Masri, S.F. (2020) 'A review on computational intelligence for identification of nonlinear dynamical systems', *Nonlinear Dynamics*, Vol. 99, pp.1709–1761 [online] <https://doi.org/10.1007/s11071-019-05430-7>.
- Radcliffe, N.J. (1991) 'Equivalence class analysis of genetic algorithms', *Complex Systems*, Vol. 5, No. 2, pp.183–205.
- Rakotondrabe, M. (2011) 'Bouc-Wen modeling and inverse multiplicative structure to compensate hysteresis nonlinearity in piezoelectric actuators', *IEEE Transactions on Automation Science and Engineering*, Vol. 8, No. 2, pp.428–431 [online] <https://doi.org/10.1109/TASE.2010.2081979>.
- Rakotondrabe, M. (2012) 'Classical Prandtl-Ishlinskii modeling and inverse multiplicative structure to compensate hysteresis in piezoactuators', in *American Control Conference (ACC)*, Montreal, QC, Canada, pp.1646–1651 [online] <https://doi.org/10.1109/ACC.2012.6314620>.
- Rakotondrabe, M. (2013) *Smart Materials-Based Actuators at the Micro/Nano-Scale: Characterization, Control and Applications*, Springer, New York [online] <https://doi.org/10.1007/978-1-4614-6684-0>.
- Rakotondrabe, M., Clévy, C. and Lutz, P. (2010) 'Complete open loop control of hysteretic, creeped, and oscillating piezoelectric cantilevers', *IEEE Transactions on Automation Science and Engineering*, Vol. 7, No. 3, pp.440–450 [online] <https://doi.org/10.1109/TASE.2009.2028617>.
- Retes, P.F.L. and Aguirre, L.A. (2019) 'NARMAX model identification using a randomised approach', *International Journal of Modelling, Identification and Control*, Vol. 31, No. 3, pp.205–216 [online] <https://doi.org/10.1504/IJMIC.2019.098779>.
- Ribeiro, A.H., Tiels, K., Umenberger, J., Schön, T.B. and Aguirre, L.A. (2020) 'On the smoothness of nonlinear system identification', *Automatica*, Vol. 121, p.109158 [online] <https://doi.org/10.1016/j.automatica.2020.109158>.
- Riccardi, L., Naso, D., Turchiano, B. and Janocha, H. (2013) 'LMI-based design of linear controllers for a magnetic shape memory push-push actuator', in *52nd IEEE Conference on Decision and Control*, Florence, Italy, pp.6634–6639 [online] <https://doi.org/10.1109/CDC.2013.6760939>.
- Riccardi, L., Naso, D., Turchiano, B. and Janocha, H. (2014) 'Design of linear feedback controllers for dynamic systems with hysteresis', *IEEE Transactions on Control Systems Technology*, Vol. 22, No. 4, pp.1268–1280 [online] <https://doi.org/10.1109/TCST.2013.2282661>.
- Riccardi, L., Naso, D., Turchiano, B., Janocha, H. and Schlueter, K. (2012) 'PID control of linear systems with an input hysteresis described by Prandtl-Ishlinskii models', in *51st IEEE Conference on Decision and Control (CDC)*, Maui, HI, USA, pp.5158–5163 [online] <https://doi.org/10.1109/CDC.2012.6425926>.
- Rodriguez-Vazquez, K., Fonseca, C.M. and Fleming, P.J. (2004) 'Identifying the structure of nonlinear dynamic systems using multiobjective genetic programming', *IEEE Transactions on Systems, Man, and Cybernetics-Part A: Systems and Humans*, Vol. 34, No. 4, pp.531–545 [online] <https://doi.org/10.1109/TSMCA.2004.826299>.
- Romano, R.A. and Garcia, C. (2011) 'Valve friction and nonlinear process model closed-loop identification', *Journal of Process Control*, Vol. 21, No. 4, pp.667–677 [online] <https://doi.org/10.1016/j.jprocont.2010.11.009>.
- Ruderman, M. and Bertram, T. (2010) 'Discrete dynamic Preisach model for robust inverse control of hysteresis systems', in *49th IEEE Conference on Decision and Control*, Atlanta, GA, USA, pp.3463–3468 [online] <https://doi.org/10.1109/CDC.2010.5717758>.
- Safari, M.J.S. and Mehr, A.D. (2018) 'Multigene genetic programming for sediment transport modeling in sewers for conditions of non-deposition with a bed deposit', *International Journal of Sediment Research*, Vol. 33, No. 3, pp.262–270 [online] <https://doi.org/10.1016/j.ijscr.2018.04.007>.
- Sain, P., Sain, M., Spencer, B. and Sain, J. (1998) 'The Bouc hysteresis model: an initial study of qualitative characteristics', in *Proceedings of the American Control Conference*, Philadelphia, PA, USA, pp.2559–2563 [online] <https://doi.org/10.1109/ACC.1998.703096>.
- Salapaka, S., Sebastian, A., Cleveland, J.P. and Salapaka, M.V. (2002) 'High bandwidth nano-positioner: a robust control approach', *Review of Scientific Instruments*, Vol. 73, No. 9, pp.3232–3241 [online] <https://doi.org/10.1063/1.1499533>.
- Schindel, D. and Aschemann, H. (2013) 'Comparison of cascaded backstepping control approaches with hysteresis compensation for a linear axis with pneumatic muscles', *IFAC Proceedings Volumes*, Vol. 46, No. 23, pp.773–778 [online] <https://doi.org/10.3182/20130904-3-FR-2041.00132>.
- Schoukens, J. and Ljung, L. (2019) 'Nonlinear system identification: a user-oriented road map', *IEEE Control Systems Magazine*, Vol. 39, No. 6, pp.28–99 [online] <https://doi.org/10.1109/MCS.2019.2938121>.
- Shakiba, S., Zakerzadeh, M.R. and Ayati, M. (2018) 'Experimental characterization and control of a magnetic shape memory alloy actuator using the modified generalized rate-dependent Prandtl-Ishlinskii hysteresis model', *Proceedings of the Institution of Mechanical Engineers, Part I: Journal of Systems and Control Engineering*, Vol. 232, No. 5, pp.506–518 [online] <https://doi.org/10.1177/0959651818758910>.
- Shen, J.-C., Jywe, W.-Y., Chiang, H.-K. and Shu, Y.-L. (2008) 'Precision tracking control of a piezoelectric-actuated system', *Precision Engineering*, Vol. 32, No. 2, pp.71–78 [online] <https://doi.org/10.1016/j.precisioneng.2007.04.002>.
- Shi, Z.-K. and Wu, F.-X. (2013) 'Robust identification method for nonlinear model structures and its application to high-performance aircraft', *International Journal of Systems Science*, Vol. 44, No. 6, pp.1040–1051 [online] <https://doi.org/10.1080/00207721.2011.652225>.
- Sjöberg, J., Zhang, Q., Ljung, L., Benveniste, A., Delyon, B., Gorenne, P-Y., Hjalmarsson, H. and Juditsky, A. (1995) 'Nonlinear black-box modeling in system identification: a unified overview', *Automatica*, Vol. 31, No. 12, pp.1691–1724 [online] [https://doi.org/10.1016/0005-1098\(95\)00120-8](https://doi.org/10.1016/0005-1098(95)00120-8).

- Smyth, A.W., Masri, S.F., Kosmatopoulos, E.B., Chassiakos, A.G. and Caughey, T.K. (2002) ‘Development of adaptive modeling techniques for non-linear hysteretic systems’, *International Journal of Non-Linear Mechanics*, Vol. 37, No. 8, pp.1435–1451 [online] [https://doi.org/10.1016/S0020-7462\(02\)00031-8](https://doi.org/10.1016/S0020-7462(02)00031-8).
- Song, G., Zhao, J., Zhou, X. and Abreu-Garcia, J.A.D. (2005) ‘Tracking control of a piezoceramic actuator with hysteresis compensation using inverse Preisach model’, *IEEE/ASME Transactions on Mechatronics*, Vol. 10, No. 2, pp.198–209 [online] <https://doi.org/10.1109/TMECH.2005.844708>.
- Stebel, K. and Czecot, J. (2009) ‘Nonstationary modelling approaches of neutralization process for model-based control’, *IFAC Proceedings Volumes*, Vol. 42, No. 13, pp.302–307 [online] <https://doi.org/10.3182/20090819-3-PL-3002.00053>.
- Sun, L., Liu, X., Chen, T., Yan, M. and Ma, S. (2021) ‘Convergence analysis of cuckoo search algorithm based on martingale theory’, *International Journal of Modelling, Identification and Control*, Vol. 39, No. 2, pp.128–137 [online] <https://doi.org/10.1504/IJMIC.2021.123431>.
- Swevers, J., Al-Bender, F., Ganseman, C. and Projogo, T. (2000) ‘An integrated friction model structure with improved presliding behavior for accurate friction compensation’, *IEEE Transactions on Automatic Control*, Vol. 45, No. 4, pp.675–686 [online] <https://doi.org/10.1109/9.847103>.
- Tan, Y. and Deng, L. (2014) ‘Modeling the dynamic sandwich system with hysteresis using NARMAX model’, *Mathematics and Computers in Simulation*, Vol. 97, pp.162–188 [online] <https://doi.org/10.1016/j.matcom.2013.04.029>.
- Tao, G. and Kokotovic, P.V. (1995) ‘Adaptive control of plants with unknown hystereses’, *IEEE Transactions on Automatic Control*, Vol. 40, No. 2, pp.200–212 [online] <https://doi.org/10.1109/9.341778>.
- Tavares, L.A., Abreu, P.E.O.G.B. and Aguirre, L.A. (2021) ‘Input design and recommendations for the identification of hysteretic NARX models’, in *Anais do XV Simpósio Brasileiro de Automação Inteligente*, Rio Grande, Brazil [online] <https://doi.org/10.20906/sbai.v1i1.2576>.
- Tavares, L.A., Abreu, P.E.O.G.B. and Aguirre, L.A. (2022) ‘Nonlinearity compensation based on identified NARX polynomials models’, *Nonlinear Dynamics*, Vol. 107, pp.709–725 [online] <https://doi.org/10.1007/s11071-021-06797-2>.
- Trivedi, G. and Rawat, T.K. (2022) ‘Volterra series based nonlinear system identification methods and modelling capabilities’, *International Journal of Modelling, Identification and Control*, Vol. 41, No. 3, pp.222–230 [online] <https://doi.org/10.1504/IJMIC.2022.127513>.
- Visintin, A. (1994) *Differential Models of Hysteresis*, Springer, Berlin, Heidelberg [online] <https://doi.org/10.1007/978-3-662-11557-2>.
- Visone, C. (2008) ‘Hysteresis modelling and compensation for smart sensors and actuators’, *Journal of Physics: Conference Series*, Vol. 138, No. 1, p.12028 [online] <http://dx.doi.org/10.1088/1742-6596/138/1/012028>.
- Wang, D.H. and Zhu, W. (2011) ‘A phenomenological model for pre-stressed piezoelectric ceramic stack actuators’, *Smart Materials and Structures*, Vol. 20, No. 3, p.35018 [online] <http://dx.doi.org/10.1088/0964-1726/20/3/035018>.
- Wang, D.H., Zhu, W. and Yang, Q. (2011) ‘Linearization of stack piezoelectric ceramic actuators based on Bouc-Wen model’, *Journal of Intelligent Material Systems and Structures*, Vol. 22, No. 5, pp.401–413 [online] <https://doi.org/10.1177/1045389X10386132>.
- Wang, G., Yao, X., Cui, J., Yan, Y., Dai, J. and Zhao, W. (2020) ‘A novel piezoelectric hysteresis modeling method combining LSTM and NARX neural networks’, *Modern Physics Letters B*, Vol. 34, No. 28, p.2050306 [online] <https://doi.org/10.1142/S0217984920503066>.
- Wang, H. and Song, G. (2014) ‘Innovative NARX recurrent neural network model for ultra-thin shape memory alloy wire’, *Neurocomputing*, Vol. 134, pp.289–295 [online] <https://doi.org/10.1016/j.neucom.2013.09.050>.
- Wei, H.L. and Billings, S.A. (2008) ‘Model structure selection using an integrated forward orthogonal search algorithm interfered with squared correlation and mutual information’, *International Journal of Modelling, Indetification and Control*, Vol. 3, No. 4, pp.341–356 [online] <https://doi.org/10.1504/IJMIC.2008.020543>.
- Wei, W., Cai, X. and Min, Z. (2021) ‘Disturbance rejection decoupling control for a wastewater treatment process’, *International Journal of Modelling, Identification and Control*, Vol. 39, No. 1, pp.39–50 [online] <https://doi.org/10.1504/IJMIC.2021.123377>.
- Wei, Z., Xiang, B.L. and Ting, R.X. (2014) ‘Online parameter identification of the asymmetrical Bouc-Wen model for piezoelectric actuators’, *Precision Engineering*, Vol. 38, No. 4, pp.921–927 [online] <https://doi.org/10.1016/j.precisioneng.2014.06.002>.
- Wen, Y.K. (1976) ‘Method for random vibration of hysteretic systems’, *Journal of the Engineering Mechanics Division*, Vol. 102, No. 2, pp.249–263 [online] <https://doi.org/10.1061/JMCEA3.0002106>.
- Worden, K. and Barthorpe, R.J. (2012) ‘Identification of hysteretic systems using NARX models, part I: evolutionary identification’, in Simmermacher, T., Cogan, S., Horta, L. and Barthorpe, R. (Eds.): *Topics in Model Validation and Uncertainty Quantification*, Vol. 4, pp.49–56, Springer [online] https://doi.org/10.1007/978-1-4614-2431-4_5.
- Worden, K. and Hensman, J.J. (2012) ‘Parameter estimation and model selection for a class of hysteretic systems using Bayesian inference’, *Mechanical Systems and Signal Processing*, Vol. 32, pp.153–169 [online] <https://doi.org/10.1016/j.ymssp.2012.03.019>.
- Worden, K., Wong, C.X., Parlitz, U., Hornstein, A., Engster, D., Tjahjowidodo, T., Al-Bender, F., Rizos, D.D. and Fassois, S.D. (2007) ‘Identification of pre-sliding and sliding friction dynamics: grey box and black-box models’, *Mechanical Systems and Signal Processing*, Vol. 21, No. 1, pp.514–534 [online] <https://doi.org/10.1016/j.ymssp.2005.09.004>.
- Xu, Q. and Li, Y. (2009) ‘Dynamics modeling and sliding mode control of an XY micropositioning stage’, in *The 9th International Symposium on Robot Control (SYROCO)*, Nagaragawa Convention Center, Gifu, Japan, pp.781–786.
- Yi, S., Yang, B. and Meng, G. (2019) ‘Ill-conditioned dynamic hysteresis compensation for a low-frequency magnetostrictive vibration shaker’, *Nonlinear Dynamics*, Vol. 96, No. 1, pp.535–551 [online] <https://doi.org/10.1007/s11071-019-04804-1>.
- Yu, Y., Xiao, Z., Naganathan, N.G. and Dukkipati, R.V. (2002) ‘Dynamic Preisach modelling of hysteresis for the piezoceramic actuator system’, *Mechanism and Machine Theory*, Vol. 37, No. 1, pp.75–89 [online] [https://doi.org/10.1016/S0094-1144\(01\)00060-X](https://doi.org/10.1016/S0094-1144(01)00060-X).

- Zakerzadeh, M.R., Sayyaadi, H. and Zanjani, M.A.V. (2011) ‘Characterizing hysteresis nonlinearity behavior of SMA actuators by Krasnosel'skii-Pokrovskii model’, *Applied Mathematics*, Vol. 1, No. 1, pp.28–38 [online] <http://dx.doi.org/10.5923/j.am.20110101.04>.
- Zhang, X., Tan, Y., Su, M. and Xie, Y. (2010) ‘Neural networks based identification and compensation of rate-dependent hysteresis in piezoelectric actuators’, *Physica B: Condensed Matter*, Vol. 405, No. 12, pp.2687–2693 [online] <https://doi.org/10.1016/j.physb.2010.03.050>.
- Zhang, W., Zhu, J. and Gu, D. (2017a) ‘Identification of robotic systems with hysteresis using nonlinear autoregressive exogenous input models’, *International Journal of Advanced Robotic Systems*, Vol. 14, No. 3, pp.1–10 [online] <https://doi.org/10.1177/1729881417705845>.
- Zhang, Y., Yan, P. and Zhang, Z. (2017b) ‘Robust adaptive backstepping control for piezoelectric nano-manipulating systems’, *Mechanical Systems and Signal Processing*, Vol. 83, pp.130–148 [online] <https://doi.org/10.1016/j.ymssp.2016.06.002>.
- Zheng, J., Wang, Q. and Li, Y. (2014) ‘Adaptive sliding model control for linear actuator with hysteresis using a Prandtl-Ishlinskii model’, in *IEEE International Conference on Robotics and Biomimetics (ROBIO 2014)*, pp.2553–2557, Bali, Indonesia [online] <https://doi.org/10.1109/ROBIO.2014.7090725>.
- Zhou, J. and Wen, C. (2008) *Adaptive Backstepping Control of Uncertain Systems: Nonsmooth Nonlinearities, Interactions or Time-Variations*, Springer, Berlin, Heidelberg [online] <https://doi.org/10.1007/978-3-540-77807-3>.
- Zhou, J., Wen, C. and Li, T. (2012) ‘Adaptive output feedback control of uncertain nonlinear systems with hysteresis nonlinearity’, *IEEE Transactions on Automatic Control*, Vol. 57, No. 10, pp.2627–2633 [online] <https://doi.org/10.1109/TAC.2012.2190208>.
- Zhou, J., Wen, C. and Zhang, Y. (2004) ‘Adaptive backstepping control of a class of uncertain nonlinear systems with unknown backlash-like hysteresis’, *IEEE Transactions on Automatic Control*, Vol. 49, No. 10, pp.1751–1759 [online] <https://doi.org/10.1109/TAC.2004.835398>.
- Zhu, Q., Li, L., Zhang, W. and Li, S. (2018) ‘Control of complex nonlinear dynamic rational systems’, *Complexity* [online] <http://dx.doi.org/10.1155/2018/8953035>.
- Zhu, Q., Wang, Y., Zhao, D., Li, S. and Billings, S.A. (2015) ‘Review of rational (total) nonlinear dynamic system modelling, identification, and control’, *International Journal of Systems Science*, Vol. 46, No. 12, pp.2122–2133 [online] <https://doi.org/10.1080/00207721.2013.849774>.

Notes

- 1 <https://github.com/CastroHc/MGGP>.
- 2 https://www.researchgate.net/publication/344269414_Identification_and_nonlinearity_compensation_of_hysteresis_using_NARX_models.